Journal of Medicinal Chemistry

ARTICLE

pubs.acs.org/jmc

Inhalation by Design: Novel Tertiary Amine Muscarinic M_3 Receptor Antagonists with Slow Off-Rate Binding Kinetics for Inhaled Once-Daily Treatment of Chronic Obstructive Pulmonary Disease

Paul A. Glossop,[*,†] Christine A. L. Watson,[*,†] David A. Price,[†,#] Mark E. Bunnage,[†] Donald S. Middleton,[†] Anthony Wood,[†,¥] Kim James,[†,Δ] Dannielle Roberts,[†] Ross S. Strang,[†] Michael Yeadon,[‡] Christelle Perros-Huguet,[‡,§] Nicholas P. Clarke,[‡,▽] Michael A. Trevethick,[‡] Ian Machin,[‡] Emilio F. Stuart,[‡] Steven M. Evans,[‡] Anthony C. Harrison,[§] David A. Fairman,[§,∥] Balaji Agoram,[§,∥] Jane L. Burrows,[⊥] Neil Feeder,[⊥] Craig K. Fulton,[⊥] Barry R. Dillon,[⊥] David A. Entwistle,[⊥] and Fiona J. Spence[▽]

[†]Department of Worldwide Medicinal Chemistry, [‡]Allergy and Respiratory Research Unit, [§]Department of Pharmacokinetics, Dynamics and Metabolism, [⊥]Department of Pharmaceutical Sciences, and [▽]Department of Drug Safety, Pfizer Global Research and Development, Sandwich Laboratories, Ramsgate Road, Kent CT13 9NJ, U.K.

Supporting Information

ABSTRACT: A novel tertiary amine series of potent muscarinic M_3 receptor antagonists are described that exhibit potential as inhaled long-acting bronchodilators for the treatment of chronic obstructive pulmonary disease. Geminal dimethyl functionality present in this series of compounds confers very long dissociative half-life (slow off-rate) from the M_3 receptor that mediates very long-lasting smooth muscle relaxation in guinea pig tracheal strips. Optimization of pharmacokinetic properties was achieved by combining rapid oxidative clearance with targeted introduction of a phenolic moiety to secure rapid glucuronidation. Together, these attributes minimize systemic exposure following inhalation, mitigate potential drug−drug interactions, and reduce systemically mediated adverse events. Compound **47** (PF-3635659) is identified as a Phase II clinical candidate from this series with in vivo duration of action studies confirming its potential for once-daily use in humans.

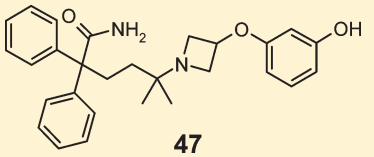

47

INTRODUCTION

Chronic obstructive pulmonary disease (COPD) is characterized by airflow limitation that is both progressive and not fully reversible, resulting in deterioration of lung function and chronic dyspnea.[1] The airflow limitation is associated with an abnormal inflammatory response to noxious particles, often developing in smokers. COPD is currently the fourth largest cause of death in the U.S. and is projected to become the third leading cause of death worldwide by 2020.[1] Bronchodilator drugs are commonly used to manage the symptoms of COPD, maximize lung function, and reduce exacerbation rates. Inhaled muscarinic receptor antagonists such as ipratropium bromide and tiotropium bromide[2] (Chart 1) are examples of one class of bronchodilators prescribed for symptom control. Ipratropium bromide is a short-acting agent administered four times per day, whereas tiotropium bromide (Spiriva) is administered once-daily, for example, from the HandiHaler capsule-based dry powder inhaler (DPI). Tiotropium is classed as a long-acting muscarinic antagonist (LAMA) or long-acting anticholinergic (LAAC).

By definition, anticholinergic agents are particularly effective because they prevent acetylcholine-induced airway smooth muscle contraction, an overall effect manifested in the lungs as bronchodilation. Cholinergic tone is therefore highly relevant and acknowledged as the major reversible component of airflow obstruction in COPD.[3] Five distinct muscarinic acetylcholine receptors (M_1−M_5) are known in humans, three of which are present in human lung (M_1−M_3). The M_3 receptor is located on airway smooth-muscle cells where it mediates the contractile response.[4]

A major area of current effort in the respiratory field is identification of novel long-acting muscarinic antagonists that provide inhaled once-daily bronchodilatory efficacy with potential for improved therapeutic index (TI) versus systemically driven adverse events such as tachycardia and dry mouth.[5,6] An agent of this type would have value as either a stand-alone therapy or for use in combination products with other once-daily bronchodilator and/or anti-inflammatory agents.[7] Reports in the literature have described numerous chemical series that offer promise against these objectives, although to date, none of these compounds have received regulatory approval as new once-daily inhaled agents.[6,8] Novel quaternary ammonium agents from these efforts include darotropium bromide (GSK233705B)[9] and aclidinium bromide (LAS-34273).[10,11] Marketed quaternary ammonium oral agents reformulated for inhaled delivery include glycopyrronium bromide (NVA-237)[6,7,12] and trospium chloride (ALKS-27).[6] These four clinical agents have progressed to phase II or phase III trials in COPD (Chart 2).

Received: July 6, 2011
Published: August 29, 2011

dx.doi.org/10.1021/jm200884j | J. Med. Chem. 2011, 54, 6888–6904

In this paper we describe the application of an "inhalation by design" philosophy to the discovery of a novel tertiary amine series of muscarinic receptor antagonists that combine the pharmacology required for once-daily inhaled administration, with pharmacokinetics designed to minimize systemic exposure and provide potential for improved therapeutic index versus systemically driven adverse events.

CHEMISTRY

Our carboxamide target compounds were prepared across three chemical series: pyrrolidines, piperidines, and azetidines. The pyrrolidine lead **4** was prepared by initial nucleophilic addition of diphenylacetonitrile to *tert*-butyl acrylate (Scheme 1). Subsequent ester deprotection gave acid **2**, a key intermediate in the synthesis of all our target compounds. Aldehyde formation (**3**), followed by reductive amination and nitrile hydrolysis, delivered amide **4** in good overall yield.

Chart 1

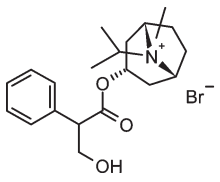

Ipratropium bromide

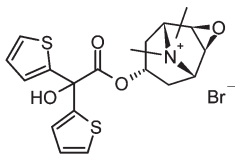

Tiotropium bromide

Chart 2

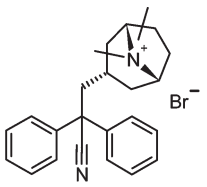

Darotropium bromide

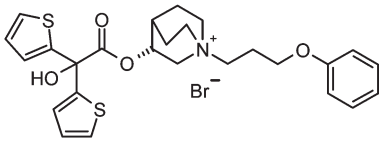

Aclidinium bromide

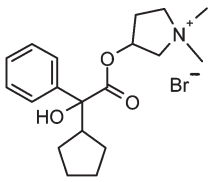

Glycopyrronium bromide

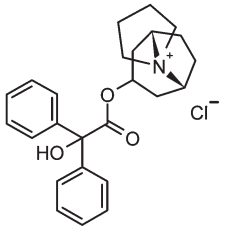

Trospium chloride

One approach to the synthesis of *gem*-dimethyl pyrrolidines is shown in Scheme 2. In this case, commercially available homochiral phenoxy-substituted pyrrolidines were coupled to an activated ester of **2**, to give amides (*R*)- and (*S*)-**5** and (*S*)-**6**. The dimethyl moiety was subsequently introduced with a modified Bouveault reaction.[13] Amides (*R*)- and (*S*)-**5** and (*S*)-**6** were treated with excess zirconium tetrachloride or titanium tetrachloride, followed by Grignard reagent, to deliver compounds (*R*)- and (*S*)-**7** and (*S*)-**8** in good yield. Hydrolysis of these nitriles with potassium hydroxide delivered amides (*R*)- and (*S*)-**9** and (*S*)-**10**. Demethylation of (*S*)-**10** with boron tribromide delivered phenol (*S*)-**11** in good yield.

An alternative strategy toward the synthesis of the pyrrolidine derivatives is shown in Scheme 3. In this approach, a late stage pyrrolidine alcohol intermediate was prepared to allow rapid analogue generation. Both (*R*)- and (*S*)-enantiomers of amide **12** could be prepared by coupling (*R*)- or (*S*)-3-benzyloxypyrrolidine to acid **2** under standard conditions. Modified Bouveault reaction followed by nitrile hydrolysis gave amides (*R*)- and (*S*)-**13** in good yield. Subsequent benzyl ether deprotection proceeded in good yield to give alcohols (*R*)- and (*S*)-**14** as key intermediates. Mitsunobu reaction was then performed with inversion of configuration to give a broad range of phenyl ether derivatives. In some cases, a biphenol was used in this reaction to provide phenol test compounds directly ((*S*)-**15**, (*S*)-**16**). In other cases, where a methyl ether protecting group was employed, test compounds were prepared by Mitsunobu reaction to give ethers ((*R*)-**10**, (*S*)-**17**, (*R*)-**18**) followed by boron tribromide deprotection to give phenols ((*R*)-**11**, (*S*)-**19**, (*R*)-**20**).

Azetidine **25** and piperidine **26** were prepared using a similar approach to that described in Scheme 2. Thus, commercially available phenoxy-substituted azetidine **21** and piperidine **22** were coupled to acid **2** to give amides **23** and **24** in good yield (Scheme 4). Subsequent Bouveault reaction and nitrile hydrolysis yielded compounds **25** and **26**.

Phenol-substituted piperidine **32** was prepared according to the route shown in Scheme 5. Boc-protected piperidine alcohol **27** was alkylated with 3-bromobenzyl bromide to give **28**, which was deprotected under acidic conditions to give amine **29** in good overall yield. Derivatization to *gem*-dimethyl intermediate **30** was accomplished under the amide coupling, Bouveault, and nitrile hydrolysis conditions already described. The benzyl ether of **30** was removed via hydrogenation to give alcohol **31**, followed by Mitsunobu reaction with resorcinol to give phenol **32**.

The ortho-substituted azetidine **35** was prepared from acid **2** and 3-(methanesulfonyl)azetidine as shown in Scheme 6. Initial coupling via the acid chloride gave mesylate **33** that was used to

Scheme 1. Synthesis of Pyrrolidine 4[a]

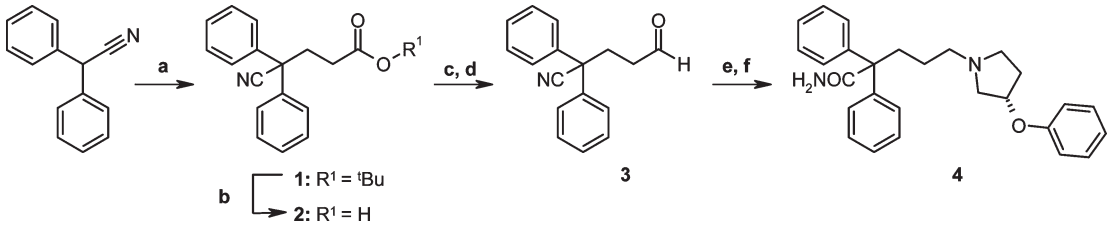

[a] Reagents: (a) ᵗButyl acrylate, KOH, MeOH, ᵗBuOH, 50 °C, 5 h, 90%; (b) 4 M HCl in 1,4-dioxane, RT, 18 h, 77%; (c) (i) CDI, THF, RT, 18 h; (ii) $NaBH_4$, RT, 18 h, 40%; (d) Dess−Martin periodinane, CH_2Cl_2, RT, 3 h, 90%; (e) (*S*)-3-phenoxypyrrolidine, $Na(OAc)_3BH$, AcOH, Et_3N, CH_2Cl_2, RT, 5 h, 47%; (f) KOH, 3-methyl-3-pentanol, reflux, 18 h, 62%.

dx.doi.org/10.1021/jm200884j |*J. Med. Chem.* 2011, 54, 6888–6904

Scheme 2. Synthesis of Pyrrolidines (*R*)- and (*S*)-9 and (*S*)-11[a]

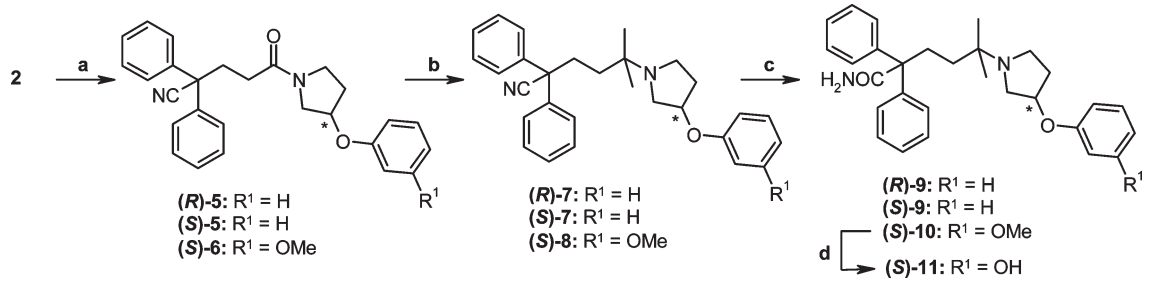

[a] Reagents: (a) (*S*)-3-phenoxypyrrolidine or (*R*)-3-phenoxypyrrolidine or (*S*)-3-(3-methoxyphenoxy)pyrrolidine, 1-hydroxybenzotriazole, 1-(3-dimethylaminopropyl)-3-ethyl carbodiimide, Et_3N, CH_2Cl_2, RT, 18 h, 41−100%; (b) $TiCl_4$, THF, −10 °C, 0.5 h; MeMgBr, −5 °C−RT, 18 h, 54%, or $ZrCl_4$, THF, −20 °C, 1 h; MeMgCl, −10 °C, 2 h, 59−78%; (c) KOH, 3-methyl-3-pentanol, reflux, 18 h, 62−96%; (d) BBr_3, CH_2Cl_2, 0 °C, 0.5 h, 60%.

Scheme 3. Synthesis of Pyrrolidines (*R*)-11, (*S*)-15, (*S*)-16, (*S*)-19, and (*R*)-20[a]

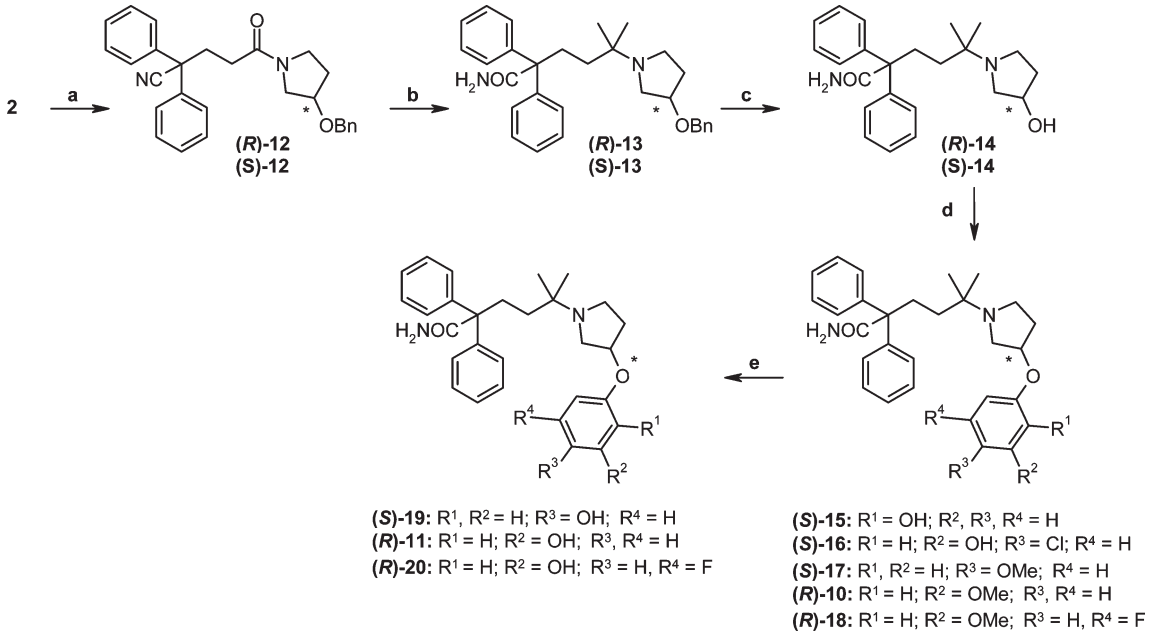

[a] Reagents: (a) (*R*)-3-benzyloxypyrrolidine, CDI, THF, RT, 18 h, 83%, or (*S*)-3-benzyloxypyrrolidine, 1-hydroxybenzotriazole, 1-(3-dimethylaminopropyl)-3-ethyl carbodiimide, Et_3N, CH_2Cl_2, RT, 18 h, 70%; (b) (i) $ZrCl_4$, THF, −20 °C, 1 h; MeMgCl, −10 °C, 2 h, 76% (ii) KOH, 3-methyl-3-pentanol, reflux, 24 h, 78−89%; (c) $FeCl_3$, CH_2Cl_2, RT, 3 h, 60%, or 20% $Pd(OH)_2$/C, 1 M HCl, EtOH, H_2, 50 psi, 50 °C, 28 h, 90%; (d) ArOH, PPh_3, DIAD, THF, 0 °C−RT, 2−22 h, 75−7%; (e) BBr_3, CH_2Cl_2, RT, 18 h, 46−68%.

Scheme 4. Synthesis of Azetidine 25 and Piperidine 26[a]

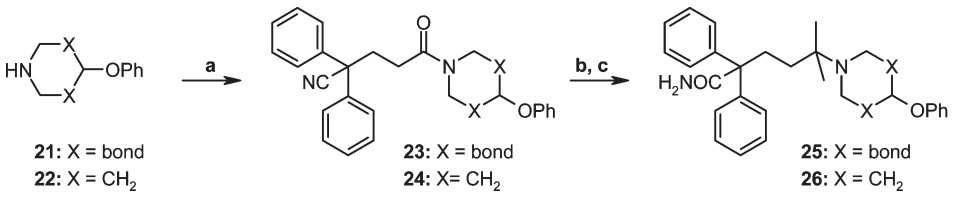

[a] Reagents: (a) **2**, 1-hydroxybenzotriazole, 1-(3-dimethylaminopropyl)-3-ethyl carbodiimide, Et_3N, DMF, RT, 18 h, 75−95%; (b) (i) $ZrCl_4$, THF, −20 °C, 1 h; (ii) MeMgCl, −10 °C, 2 h, 38−41%; (c) KOH, 3-methyl-3-pentanol, reflux, 18 h, 88−93%.

alkylate 2-(benzyloxy)phenol. Subsequent Bouveault reaction proceeded in poor yield in this case, but still afforded *gem*-dimethyl azetidine **34**. Nitrile hydrolysis and hydrogenation of the benzyl protecting group afforded phenol **35**.

The low yield of the modified Bouveault reaction led us to seek an alternative method for the introduction of the *gem*-dimethyl group in the azetidine series. Synthesis began with Boc-protected oxathiazinane dioxide **36** (Scheme 7).[14] Ring-opening of protected

dx.doi.org/10.1021/jm200884j |*J. Med. Chem.* 2011, 54, 6888–6904

Scheme 5. Synthesis of Piperidine 32[a]

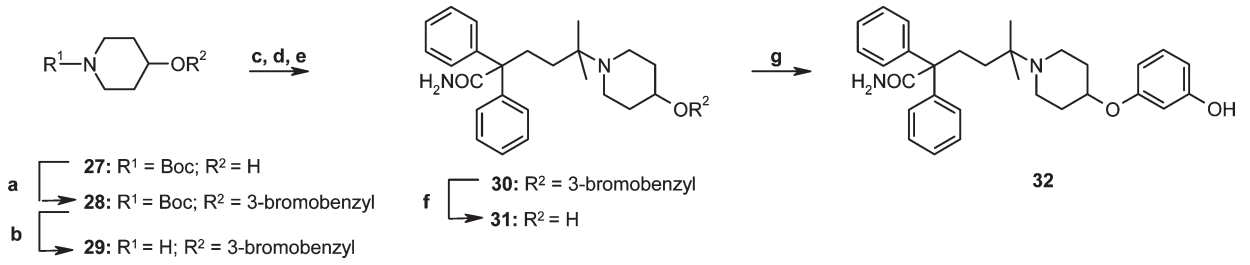

[a] Reagents: (a) NaH, 3-bromobenzyl bromide, THF, 0 °C−RT, 18 h, 61%; (b) 4 M HCl in 1,4-dioxane, RT, 2.5 h, 98%; (c) **2**, 1-hydroxybenzotriazole, 1-(3-dimethylaminopropyl)-3-ethyl carbodiimide, Et_3N, DMF, RT, 18 h, 95%; (d) (i) $ZrCl_4$, THF, −20 °C, 1 h; (ii) MeMgCl, −10 °C, 2 h, 33%; (e) KOH, 3-methyl-3-pentanol, reflux, 18 h, 99%; (f) 20% $Pd(OH)_2/C$, 1 M HCl, EtOH, H_2, 50 psi, 50 °C, 18 h, 95%; (g) resorcinol, PPh_3, DIAD, THF, 0 °C−RT, 12 h, 14%.

Scheme 6. Synthesis of Azetidine 35[a]

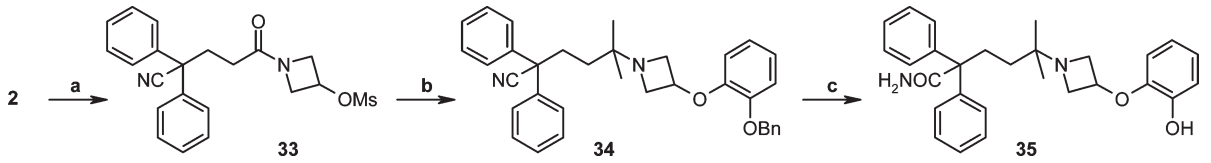

[a] Reagents: (a) (i) oxalyl chloride, DMF, CH_2Cl_2, 2 h; (ii) 3-(methanesulfonyl)azetidine, Et_3N, CH_2Cl_2, −78 °C, 1 h, 97%; (b) (i) 2-(benzyloxy) phenol, Cs_2CO_3, DMF, 80 °C, 18 h, 77%; (ii) $ZrCl_4$, THF, −35 °C, 1 h; (iii) MeMgCl, −20 °C, 1 h, 10%; (c) (i) KOH, 3-methyl-3-pentanol, reflux, 20 h, 55%; (ii) NH_4HCO_2, 20% $Pd(OH)_2/C$, EtOH, reflux, 4 h, 100%.

Scheme 7. Synthesis of Azetidines 47−53 and 55[a]

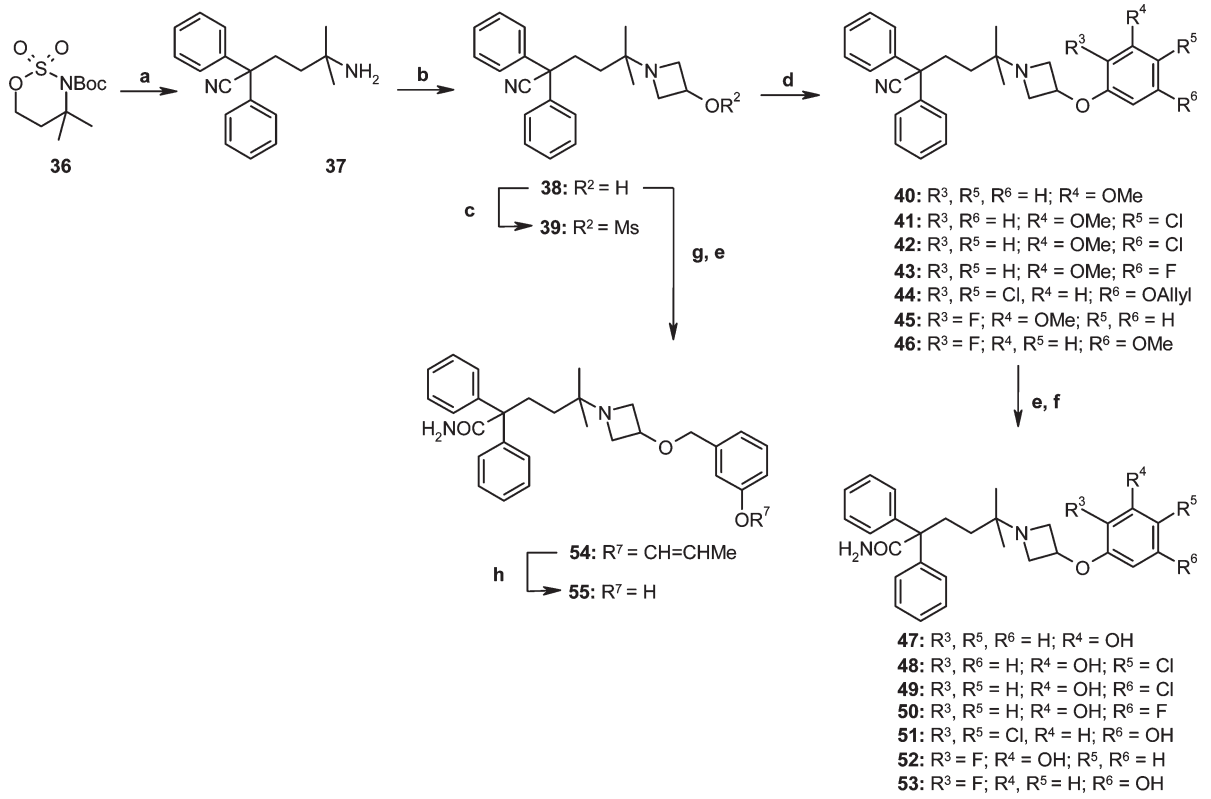

[a] Reagents: (a) (i) diphenylacetonitrile, KO^{t}Bu, THF, RT, 4 h; (ii) 4 M HCl in dioxane, 50 °C, 2 h, 87%; (b) epichlorohydrin, EtOH, 70 °C, 18 h, 79%; (c) MsCl, pyridine, −15−5 °C, 3 h, 100%; (d) ArOH, Cs_2CO_3, DMF, 80 °C, 18 h, 68−90%; (e) KOH, 3-methyl-3-pentanol, reflux, 18 h, 72−96%; (f) BBr_3, CH_2Cl_2, 0 °C, 2 h, 25−100%, or 4 M HCl in dioxane, 60 °C, 0.5 h, 61%; (g) 1-allyloxy-3-bromomethylbenzene, NaH, DMF, 0 °C, 1 h, 54%; (h) 4 M HCl in dioxane, 85 °C, 0.5 h, 70%.

dx.doi.org/10.1021/jm200884j |*J. Med. Chem.* 2011, 54, 6888–6904

Scheme 8. Synthesis of Azetidine 64[a]

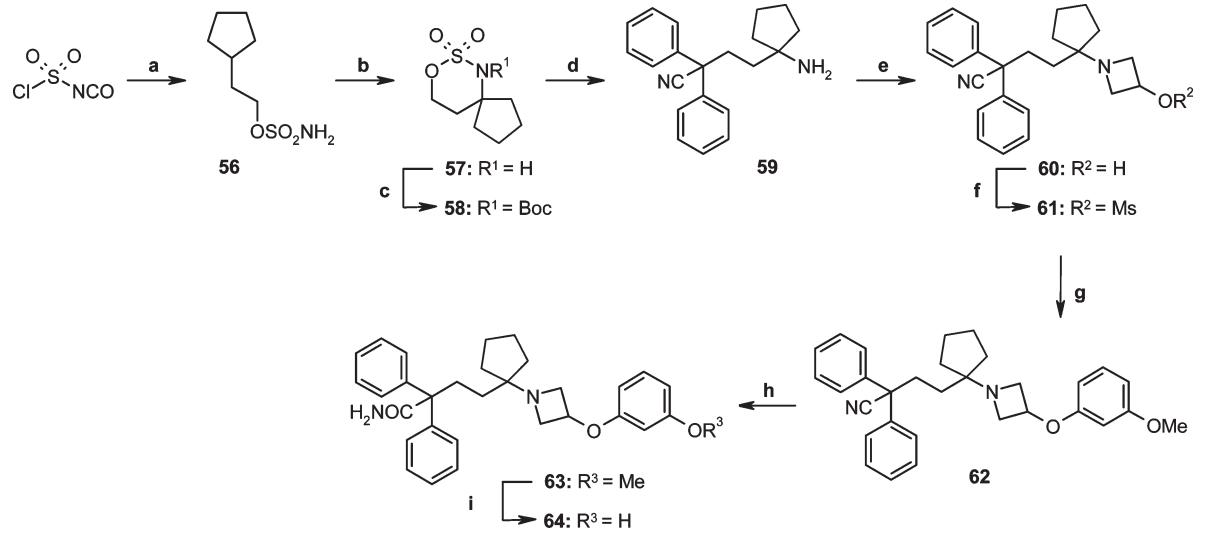

[a] Reagents: (a) (i) HCOOH, 0 °C, 0.5 h; (ii) 2-cyclopentyl ethanol, pyridine, CH_2Cl_2, < 7 °C, 2 h, 95%; (b) rhodium acetate dimer, magnesium oxide, iodobenzene diacetate, CH_2Cl_2, 18 h, 75%; (c) di-*tert*-butyl dicarbonate, Et_3N, 4-dimethylaminopyridine, CH_2Cl_2, 3 h, 46%; (d) (i) diphenylacetonitrile, KO^{t}Bu, DMF, 18 h; (ii) 4 M HCl in dioxane, 40 °C, 2 h, 67%; (e) epichlorohydrin, MeOH, 60 °C, 48 h, 52%; (f) MsCl, pyridine, −15 °C, 2 h, 59%; (g) 3-methoxyphenol, Cs_2CO_3, DMF, 80 °C, 18 h, 73%; (h) KOH, 3-methyl-3-pentanol, reflux, 20 h, 48%; (i) BBr_3, CH_2Cl_2, 0 °C, 2 h, 53%.

sulfamate esters similar to **36** has been reported using a broad range of nucleophiles including amines, acetates, azides,[15] and carbon nucleophiles such as malonate derivates and aryl-substituted enolates.[16] Gratifyingly, deprotonation of diphenylacetonitrile under basic conditions, followed by nucleophilic attack on sulfamate **36**, gave ring-opened intermediate **37**, after deprotection of the Boc group. Reaction of amine **37** with racemic epichlorohydrin delivered azetidine **38** in moderate yield, which could be converted to mesylate **39** under standard conditions. Mesylate **39** was a key intermediate that furnished a broad range of azetidine derivatives. Thus, reaction of **39** with a panel of phenols, suitably protected where appropriate, gave compounds **40**−**46** in high yield. Hydrolysis of the nitrile and removal of any protecting groups gave carboxamide derivatives **47**−**53**. Alternatively, alkylation of alcohol **38** with 1-allyloxy-3-bromomethylbenzene under basic conditions led to a benzylated intermediate that gave amide **54** after treatment with potassium hydroxide. Interestingly, potassium hydroxide led to isomerization of the allyl protecting group to give an enol ether that could be cleaved readily under acid conditions to give phenol **55**. In general, the protected phenol derivatives employed in Scheme 7 were commercially available; however, when synthesis was required, they could be prepared by monoprotection of the corresponding biphenol under standard conditions.[17]

The route to cyclopentyl derivative **64** is shown in Scheme 8. The synthesis began with conversion of 2-cyclopentyl ethanol to sulfamate ester **56** using chlorosulfonyl isocyanate and formic acid. Treatment of **56** with rhodium acetate in the presence of magnesium oxide and an oxidant resulted in C−H insertion to produce oxathiazine dioxide **57**.[15] Boc protection proceeded under standard conditions to deliver compound **58** that was subsequently converted to phenol **64** via intermediates **59**−**63**, using similar conditions to those described for the corresponding *gem*-dimethyl derivative **47** (Scheme 7).

RESULTS AND DISCUSSION

The objective of our research was to identify a long-acting muscarinic M_3 receptor antagonist with suitability for once-daily inhaled administration and pharmacokinetics consistent with minimal systemic exposure. We were confident that we would be able to apply our "inhalation by design" experience to maximize TI versus systemic muscarinic effects through careful optimization of the pharmacokinetic properties, specifically, by incorporation of a metabolically labile functional group. In contrast, strategies to incorporate long duration of action (DoA) are far less well understood. One approach reported in the field of antimuscarinics is quaternization of the tertiary amino functional group, for example, as applied in the design of aclidinium bromide.[10] However, this approach does not guarantee long DoA, as evidenced by the short-acting nature of the quaternary agent ipratropium bromide. Both aclidinium and tiotropium are known to exhibit an off-rate from the muscarinic M_3 receptor slower than that of ipratropium, and this is thought to be important in driving their long-acting effects in vivo.[18] Consequently, we decided to use targeted screening to identify a compound with a long dissociation half-life from the M_3 receptor as a strategy to secure intrinsic, sustained DoA in the lung.

Previous efforts in our laboratories had focused on the delivery of an oral muscarinic antagonist for the treatment of urinary urge incontinence and overactive bladder. This culminated in the identification of the carboxamide clinical candidate darifenacin.[19] At the start of our program to identify an inhaled candidate, we rescreened a subset of legacy muscarinic antagonists from our compound file, this time looking specifically for slow dissociation from the M_3 receptor, measured in a dilution filtration binding assay.

Under our assay conditions, both tiotropium and ipratropium had high affinity for the M_3 receptor (binding K_i = 0.075 and 0.29 nM, respectively, Table 1). The dissociation half-life of

Table 1. M_3 Functional Potency, M_3 and M_2 Binding Affinity, M_3 Dissociation Half-Life, clogP and log *D*, and HLM Clearance Data for Compounds 4, (*S*)- and (*R*)-9, 25, and 26

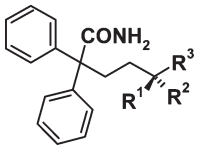

Compound	R^1	R^2	R^3	M_3 K_i[a] (nM)	M_3 K_i[b] (nM)	M_2 K_i[c] (nM)	M_3 dissociation $t_{1/2}$[d] (min)	clogP/ log *D*	HLM Cl_{int}[e] (μL/min)/mg
4	H	H	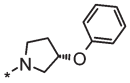	2.4	1.9	15	38	4.2 -	ND[f]
(*S*)-**9**	Me	Me	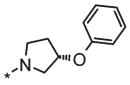	0.25	1.8	1.6	>1440	5.0 2.9	>440
(*R*)-**9**	Me	Me	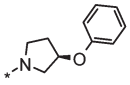	1.6	6.4	12	>1440	5.0 -	ND[f]
25	Me	Me	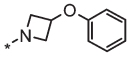	0.049	0.11	0.056	481	5.0 3.5	>440
26	Me	Me	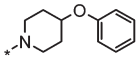	0.27	3.9	2.6	1050	4.9 -	ND[f]
Tiotropium				0.051	0.075	0.061	>1440	-1.7 / -0.8	<7
Ipratropium				0.19	0.29	0.48	17	-2.2 / -0.6	<7

[a] Cell-based functional potency in CHO cells expressing recombinant human M_3 receptors. Carbamoyl choline (CCh) and test compounds were coadministered and allowed to equilibrate for 4 h. Compound inhibition of CCh stimulated calcium currents was measured. All compounds appeared to be full antagonists in this assay. Determinations were the mean of at least two replicates. [b] Binding affinity determined in human recombinant M_3 receptors expressed in CHO cells following incubation with [^{3}H]-NMS and test compounds for 2 h. Determinations were the mean of at least two replicates. [c] Binding affinity determined in human recombinant M_2 receptors expressed in CHO cells following incubation with [^{3}H]-NMS and test compounds for 2 h. Determinations were the mean of at least two replicates. [d] Test compound was incubated with CHO cells expressing the recombinant human M_3 receptor for 2 h at 100-fold its hM_3 binding K_i. 90-fold dilution with buffer containing excess [^{3}H]-NMS followed. The dissociation half-life of the compound was measured by monitoring the association rate of [^{3}H]-NMS. Determinations were the mean of at least four replicates. [e] Intrinsic clearance in human liver microsomes. [f] ND: not determined.

tiotropium was >1440 min, whereas ipratropium dissociated rapidly (17 min), in agreement with literature data.[2] Legacy carboxamide **4** had good binding affinity (K_i = 1.9 nM) but a relatively rapid dissociation half-life (38 min). However, *gem*-dimethyl substitution adjacent to the basic amine moiety had a profound effect on the rate of dissociation. Compound (*S*)-**9** had a similar binding affinity (K_i = 1.8 nM) to **4** but greatly extended dissociation half-life (>1440 min), similar to tiotropium. We speculate that dimethyl substitution may restrict conformational freedom in close proximity to the amine functional group (a key binding motif), requiring significant reordering of the ligand and receptor for binding to occur, resulting in reduced rates of association and dissociation. The enantiomer of (*S*)-**9** had a similar, exciting profile ((*R*)-**9**), albeit slightly less potent. The achiral azetidine (**25**) and piperidine (**26**) analogues also looked interesting; it appeared that the *gem*-dimethyl effect on dissociation half-life translated across different ring systems. Azetidine **25** had excellent, tiotropium-like binding affinity (K_i = 0.11 nM) and retained an encouraging dissociation half-life (481 min), while the piperidine had a profile similar to that of the pyrrolidines (*S*)- and (*R*)-**9**.

Both tiotropium and ipratropium are nonselective muscarinic antagonists, binding to the M_1−M_5 receptors with approximately equal affinity.[18] Compounds representing our novel carboxamide series were also shown to be nonselective muscarinic antagonists when tested against the M_2 receptor (Table 1), which we deemed to be the most relevant initial counter-screen due to the potential for M_2-mediated tachycardia. Data against the M_1, M_4, and M_5 receptors were not gathered at this stage. All compounds tested were full M_3 antagonists in a functional cell-based assay where inhibition of carbamyl choline-stimulated calcium currents was measured. The potency of the carboxamide series in this functional assay was found to be broadly equivalent to affinity in the filtration binding experiment (Table 1).

Compounds (*S*)- and (*R*)-**9**, **25**, and **26** gave us confidence that slow dissociation from the M_3 receptor and potential for

dx.doi.org/10.1021/jm200884j |*J. Med. Chem.* 2011, 54, 6888–6904

Table 2. M_3 Functional Potency, M_3 Dissociation Half-Life, clogP and log *D*, and in Vitro Clearance Data for Phenolic Compounds (*R*)- and (*S*)-11, (*S*)-15, (*S*)-19, 32, 35, 47, 55, and 64

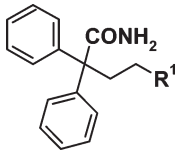

Compound	R^1	M_3 K_i[a] (nM)	M_3 dissociation $t_{1/2}$[b] (min)	clogP/ log *D*	HLM Cl_{int}[c] (μL/min)/mg	HHeps Cl_{int}[d] (μL/min)/million	Gluc Cl_{int}[e] (μL/min)/mg
(*R*)-**11**	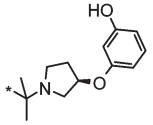	0.51	>1440	4.5 2.6	>440	67	82
(*S*)-**11**	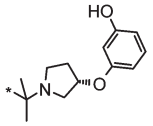	0.21	>1440	4.5 2.4	>440	65	52
(*S*)-**15**	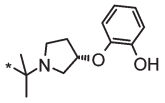	0.16	387	4.2 2.3	>440	30	13
(*S*)-**19**	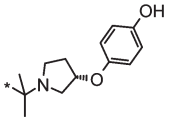	0.76	229	4.5 -	ND[f]	ND[f]	<4
32	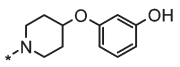	2.3	>1440	4.4 2.6	187	15	ND[f]
35	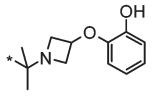	11	ND[f]	4.3 2.9	>440	64	ND[f]
47	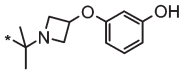	0.20	>1440	4.6 3.0	>282	96	221
55	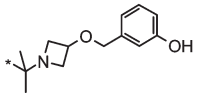	0.18	1240	4.5 2.1	364	34	13
64	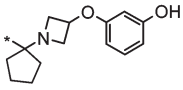	0.73	>1440	5.2 -	308	121	143
	(*S*)-**9**	0.25	>1440	5.0 / 2.9	>440	23	ND[f]
	Tiotropium	0.051	>1440	-1.7 / -0.8	<7	<5	ND[f]

[a] Cell based functional potency in CHO cells expressing recombinant human M_3 receptors. Carbamoyl choline (CCh) and test compounds were coadministered and allowed to equilibrate for 4 h. Compound inhibition of CCh stimulated calcium currents was measured. All compounds appeared to be full antagonists in this assay. Determinations were the mean of at least two replicates. [b] Test compound was incubated with CHO cells expressing the recombinant human M_3 receptor for 2 h at 100-fold its hM_3 binding K_i. 90-fold dilution with buffer containing excess [^{3}H]-NMS followed. The dissociation half-life of the compound was measured by monitoring the association rate of [^{3}H]-NMS. Determinations were the mean of at least four replicates. [c] Intrinsic clearance in human liver microsomes activated with NADPH. [d] Intrinsic clearance in human hepatocytes. [e] Intrinsic clearance in human liver microsomes treated with Brij-58 and UDPGA. [f] ND: not determined.

long DoA was achievable in our *gem*-dimethyl-substituted carboxamides. Attention then turned to optimization of the pharmacokinetic properties to maximize TI. Inhaled anticholinergics are associated with a range of side effects related to systemic exposure including dry mouth, constipation, glaucoma, urinary retention, and cardiovascular effects. Consequently, we aimed to

minimize such systemic effects through reduced oral bioavailability (of the swallowed fraction of the dose) and high clearance of the inhaled dose.

Quaternary muscarinic antagonists have low oral bioavailability, largely as a consequence of reduced absorption due to their polarity.[6] Both tiotropium and ipratropium have log D < 1 (Table 1), resulting in reduced membrane permeability and low oral absorption that drives low systemic exposure of the swallowed fraction of the dose. In contrast, our carboxamides leads (*S*)- and (*R*)-**9**, **25**, and **26** possessed high clogP and moderate log D and would therefore be expected to have good membrane permeability and be well absorbed. Compound (*S*)-**9** was typical, with a moderate cell permeability and no evidence of transporter-mediated efflux (P_{app}(A−B) = 16 × 10^{-6} cm/s, P_{app}(B−A) = 13 × 10^{-6} cm/s), measured by apical to basal flux rate in Caco-2 cells. It is widely understood that absorption is only one component of oral bioavailability; first pass metabolism is also important. We therefore aimed to achieve a good TI by designing in high hepatic clearance in addition to reduced permeability. Encouragingly, (*S*)-**9** and **25** were turned over rapidly in HLM (Cl_{int} > 440 (μL/min)/mg); as expected, tiotropium and ipratropium showed high levels of microsomal stability due to their polarity, but are subject to rapid renal clearance in humans.[2]

Both the rate and route of clearance are important in determining TI across a patient population. For example, are the metabolites pharmacologically active? Which enzymes are responsible for drug clearance? A compound metabolized by only cytochrome P450 (CYP) 3A4 could be particularly vulnerable to drug−drug interactions, where a patient exposed to a CYP3A4 inhibitor (e.g., ketoconazole) would suffer from increased systemic exposure and increased muscarinic receptor-driven side effects. Interpatient variability can also be caused by genetic polymorphism, for example, CYP2D6 substrates are cleared at a significantly lower rate in certain subsets of the population (6−8% of Caucasians do not express CYP2D6).[20] We therefore sought to maximize clearance by targeting multiple clearance routes with high capacity and the lowest risk of saturation or inhibition.

Early on, we decided to target glucuronidation as a significant route of clearance for our compounds. There is little evidence of clinically relevant drug-related inhibition of glucuronidation so the risk of drug−drug interactions is low.[21] This is due to the low affinity of any inhibitors to the uridine-5′-diphosphoglucuronosyl transferase (UGT) enzymes responsible for glucuronidation and the potential for multiple UGTs to effect the glucuronidation process. Glucuronidation results in the conjugation of glucuronic acid from UDPGA (uridine-5′-diphosphoglucuronic acid) to a reactive functional group in the substrate. In this way, a lipophilic drug molecule is derivatized to a polar, water-soluble glucuronide which can be cleared by biliary or renal elimination. The chance of a pharmacologically active metabolite is therefore low. Phenols and carboxylic acids are the main substrates for UGTs, but our experience in the design of β_2-adrenoreceptor agonists led us to favor glucuronidation of phenols as our phase II clearance route.[22]

Phenolic substitution appeared to be well tolerated in some of our initial examples (Table 2). For example phenol (*S*)-**11** displayed similar, excellent M_3 functional potency (K_i = 0.21 nM) to its nonphenolic counterpart (*S*)-**9** (K_i = 0.25 nM). Importantly, the dissociation half-life of (*S*)-**11** (>1440 min) also appeared to be unaffected and the phase I clearance rate remained high (HLM Cl_{int} > 440 (μL/min)/mg), despite the lower log D (2.4 vs 2.9). The enantiomer (*R*)-**11** had a very similar profile in terms of both pharmacology and oxidative clearance. Interestingly, the location of the phenol substituent (ortho-, meta-, or para-position) had little impact on M_3 functional potency in the pyrrolidine series ((*S*)-**15**, (*S*)-**11**, (*S*)-**19**, respectively). However, ortho- and para-substitution ((*S*)-**15**, (*S*)-**19**) resulted in a drop in the dissociation half-life (387 and 229 min, respectively).

We were encouraged that our phenols were still cleared rapidly by oxidative metabolism but wanted to establish whether they were also glucuronidation substrates. One method frequently used to assess clearance via glucuronidation is the measurement of turnover of a compound in human hepatocytes. However, hepatocytes support both phase I and phase II metabolism, making it more difficult to determine the degree of non-P450-mediated clearance for compounds with rapid turnover in the standard HLM assay. Therefore, we also employed a detergent-treated (Brij-58) HLM preparation where UDPGA was added as a glucuronic acid donor to assess specific UGT metabolic activity.[23] In contrast to our standard HLM assay, no NADPH was provided in the preparation, so phase I metabolism was not supported. Brij-58 was added to allow access to the active site of the UGTs, as the metabolizing enzymes lie on the luminal side of the endoplasmic reticulum. The SAR for clearance via glucuronidation (Gluc Cl_{int}) is shown in Table 2. Once again, the enantiomeric pair (*R*)- and (*S*)-**11** had similar profiles, both demonstrating moderate clearance (52 and 82 (μL/min)/mg, respectively). In contrast, *o*- and *p*-phenols (*S*)-**15** and (*S*)-**19** did not undergo significant turnover in this assay (13 and <4 (μL/min)/mg, respectively), indicating that glucuronidation would be a minor clearance process for these compounds. The clearance in human hepatocytes revealed the same trend, with (*S*)-**15** showing a turnover (30 (μL/min)/million) lower than that for (*R*)- and (*S*)-**11** (67 and 65 (μL/min)/million, respectively).

The *m*-phenol-substituted piperidine **32** exhibited significantly reduced M_3 potency (K_i = 2.3 nM). In contrast, the azetidine core showed excellent potency and dissociation half-life with the meta-substituted phenol **47** and the benzyl analogue **55** having subnanomolar potency (K_i = 0.20 and 0.18 nM, respectively). Phenol substitution was not always tolerated by the receptor; for example, ortho-substituted azetidine **35** lost significant (55-fold) activity relative to its meta-substituted analogue (**47**). Interestingly, cyclization of the *gem*-dimethyl moiety into a cyclopentyl ring gave another potent derivative **64** (K_i = 0.73 nM) that also retained a long dissociation half-life (>1440 min). While all of the azetidine derivatives showed high levels of oxidative clearance, it was the meta-substituted phenyl ethers (**47**, **64**) that again showed the most encouraging turnover in the glucuronidation assay. Compound **47** had an excellent profile in all the in vitro assays. It possessed high affinity for the M_3 receptor (K_i = 0.20 nM), a long dissociation half-life (>1440 min), similar to tiotropium, rapid clearance in human liver microsomes (Cl_{int} > 282 (μL/min)/mg) and human hepatocytes (Cl_{int} = 96 (μL/min)/million), and very high turnover in our glucuronidation assay (Cl_{int} = 221 μL/min/mg).

The human hepatocyte assay could be used to rank compounds for phase II clearance to some degree, but the glucuronidation HLM assay clearly showed that SAR existed for glucuronidation. It was found that certain phenol derivatives were not significantly turned over by the UGTs. In some cases this might be explained by steric hindrance, for example, as with

Table 3. The Effect of Halogen Substitution on M_3 Functional Potency, M_3 Dissociation Half-Life, clogP and log *D*, in Vitro Clearance, and Calculated Acidic pK_a of Phenolic Compounds (*S*)-16, (*R*)-20, and 48−53

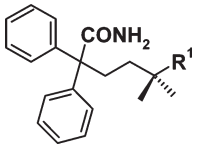

Compound	R^1	M_3 K_i[a] (nM)	M_3 dissociation $t_{1/2}$[b] (min)	clogP/ log *D*	HLM Cl_{int}[c] (μL/min)/mg	HHeps Cl_{int}[d] (μL/min)/million	Gluc Cl_{int}[e] (μL/min)/mg	Calc acidic pK_a[f]
(*S*)-**16**	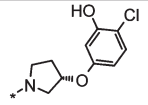	2.0	803	5.1	197	107	146	8.0
(*R*)-**20**	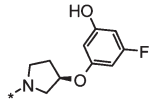	0.56	>1440	4.8 3.0	>440	114	ND[g]	8.5
48	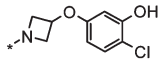	1.9	1410	5.2 -	116	159	430	7.9
49	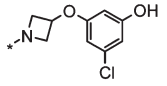	0.22	ND[g]	5.5 -	361	116	223	8.4
50	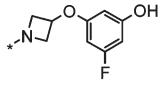	0.60	ND[g]	4.9 3.3	176	ND[g]	403	8.4
51	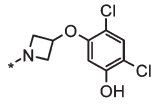	7.3	165	5.7 >4.5	115	107	186	7.5
52	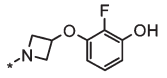	0.26	1240	4.5 3.3	451	68	52	8.1
53	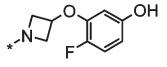	0.71	>1440	4.7 3.6	>440	159	164	9.5
	47	0.20	>1440	4.6 / 3.0	>282	96	221	9.5
	Tiotropium	0.051	>1440	-1.7 / -0.8	<7	<5	ND[g]	ND[g]

[a] Cell-based functional potency in CHO cells expressing recombinant human M_3 receptors. Carbamoyl choline (CCh) and test compounds were coadministered and allowed to equilibrate for 4 h. Compound inhibition of CCh-stimulated calcium currents was measured. All compounds appeared to be full antagonists in this assay. Determinations were the mean of at least two replicates. [b] Test compound was incubated with CHO cells expressing the recombinant human M_3 receptor for 2 h at 100-fold its hM_3 binding K_i. 90-fold dilution with buffer containing excess [^{3}H]-NMS followed. The dissociation half-life of the compound was measured by monitoring the association rate of [^{3}H]-NMS. Determinations were the mean of at least four replicates. [c] Intrinsic clearance in human liver microsomes activated with NADPH. [d] Intrinsic clearance in human hepatocytes. [e] Intrinsic clearance in human liver microsomes treated with Brij-58 and UDPGA. [f] Most acidic pK_a value calculated at 25 °C and zero ionic strength in aqueous solutions, using ACD/Physchem Batch 9.03 software from Advanced Chemistry Development, Inc. [g] ND: not determined.

the low clearance of *o*-phenol (*S*)-**15**. In other cases, it appeared to be related to structure more broadly. For example, there was a general trend for the azetidine series to exhibit higher clearance via glucuronidation than the pyrrolidine series (e.g., **47** vs (*R*)-**11**). The low clearance of benzyl derivative **55** versus phenyl analogue **47** seemed to indicate that even relatively lipophilic and sterically accessible phenols could be quite stable with respect to glucuronidation. UGTs are reported to turn over a wide array of chemical structures as a result of their important role in detoxification of endogenous compounds and xenobiotics.[24] Our data showed that structural features could be used to tune the rate of clearance up or down. Such information could also be illuminating in drug discovery programs where low clearance compounds are desired.

We were keen to investigate further structural features that could affect the rate of turnover by UGTs. Structural studies have indicated that the transfer of glucuronic acid to the phenol functional group is a base-catalyzed process where conserved

dx.doi.org/10.1021/jm200884j |*J. Med. Chem.* 2011, 54, 6888–6904

Table 4. Additional in Vitro and in Vivo Characterization of Selected Compounds (*R*)- and (*S*)-11, 47, and 52

			guinea pig trachea			
compd	M_3 binding K_i[a] (nM)	M_3 dissociation $t_{1/2}$[b] (min)	IC_{50}[c] (nM)	T_{25}[d] (h)	human bronchus pK_b[e]	guinea pig in vivo IC_{50}[f] (μg)
(*R*)-**11**	0.201	>1440	3.87 (n = 3)	>16 (n = 3)	8.0 (n = 1)	20 (n = 3)
(*S*)-**11**	0.180	>1440	4.30 (n = 4)	>16 (n = 2)	9.3 (n = 2)	10 (n = 3)
47	0.128	>1440	1.53 (n = 3)	>16 (n = 3)	9.6 (n = 3)	3 (n = 6)
52	0.163	>1440	3.48 (n = 3)	>16 (n = 2)	8.8 (n = 2)	4 (n = 4)
tiotropium	0.0098	>1370	0.41 (n = 16)	>12.9 (n = 4)	10.2 (n = 3)	0.4 (n = 10)
ipratropium	0.213	11.8	ND[g]	1.47 (n = 2)	ND[g]	ND[g]

[a] Binding affinity at human recombinant M_3 receptors expressed in CHO cells following incubation with [^{3}H]-NMS and test compound for 24 h. Determinations were the mean of at least six replicates. [b] Test compound was incubated with CHO cells expressing the recombinant human M_3 receptor for 24 h at 100-fold its hM_3 binding K_i. 90-fold dilution with buffer containing excess [^{3}H]-NMS followed. The dissociation half-life of the compound was measured by monitoring the association rate of [^{3}H]-NMS. Determinations were the mean of at least six replicates. [c] Potency in guinea pig trachea following incubation with test compound for 8 h. [d] Time taken for the EFS contractile response to recover by 25% of the inhibition induced by an E_{max} concentration of the test compound incubated for 2 h. [e] Potency in isolated human bronchial ring following incubation with test compound for 4 h. [f] Potency in an anaesthetized guinea pig model of ACh (iv)-induced bronchoconstriction, following cumulative intratracheal administration of test compound at hourly intervals, as a solution in micelle. ACh (iv) challenge was administered hourly (prior to the next escalating dose of compound), and the maximum increase in lung resistance recorded over a 5 min period, in order to produce a five-point dose−response curve. [g] ND: not determined.

carboxylate and histidine residues facilitate the deprotonation of the phenol, enabling nucleophilic attack on UDPGA.[24] We were therefore keen to investigate whether the pK_a of the phenol could be a factor in determining the rate of clearance. As meta-substituted phenols had shown the best balance of potency, dissociation half-life, and clearance (Table 2), the properties of halogen-substituted *m*-phenols were therefore explored (Table 3). In the azetidine core, the M_3 potency of chlorophenol **48** was reduced 10-fold relative to **47**, although there was little change in dissociation half-life. The additional chlorine atom resulted in increased clogP, and HLM and hepatocyte clearance remained high. In addition, the clearance by glucuronidation increased to 430 (μL/min)/mg, possibly as a result of increased clogP, but reduced pK_a could also be a factor. The calculated pK_a of the phenol of **48** was significantly lower than that of **47** (7.9 vs 9.5). The addition of a *m*-chloro substituent (**49**) also resulted in the retention of M_3 potency (K_i = 0.22 nM), high oxidative clearance (HLM Cl_{int} = 361 (μL/min)/mg), and rapid glucuronidation (Gluc Cl_{int} = 223 (μL/min)/mg). The corresponding fluorophenol **50** had a similar profile, again demonstrating very rapid glucuronidation (Cl_{int} = 403 (μL/min)/mg). Addition of a second halogen substituent (**51**) resulted in retention of the high clearance properties of the lead azetidine (**47**) but significant loss of potency (37-fold) and dissociation half-life (165 min). Fluoro substitution ortho to the phenol (**52**) resulted in a slightly reduced rate of phase II clearance (Gluc Cl_{int} = 52 (μL/min)/mg), but excellent potency (K_i = 0.26 nM) was retained. Fluorophenol isomer **53** had a similar profile to its parent azetidine (**47**), with good potency against the M_3 receptor, long dissociation half-life, and rapid phase I and phase II clearance.

In the pyrrolidine core, addition of a chloro substituent ((*S*)-**16**) resulted in reduced potency (10-fold) relative to phenol (*S*)-**11** but did provide an approximately 3-fold increase in the rate of glucuronidation (Cl_{int} = 146 (μL/min)/mg). This effect may also be due to a combination of increased clogP and reduced pK_a. The *m*-fluoro derivative (*R*)-**20** possessed good potency (K_i = 0.56 nM), a very long dissociation half-life (>1440 min), rapid clearance in HLM, and high hepatocyte clearance that indicated a high level of turnover by glucuronidation. To conclude, we were able to affect the rate of clearance of compounds in our glucuronidation assay by modification of the substituents on the phenol ring.

A selection of promising compounds ((*R*)- and (*S*)-**11**, **47**, **52**), based on a combination of pharmacology and material properties, was advanced to more comprehensive evaluation and comparison against tiotropium and ipratropium (Table 4). Following observations that these agents dissociated very slowly from the M_3 receptor (slow off-rate, small k_{off}), there was an accompanying possibility that they would demonstrate slow association (slow on-rate, small k_{on}), a rate that is a function of both ligand concentration (dose) and time.[25] This property has the potential to extend incubation times and concentrations required for an assay to reach ligand−receptor equilibrium and accurately define the equilibrium dissociation constant (K_d). In response to these observations, M_3 binding affinity (K_i) was determined for the selected compounds in revised assay conditions requiring incubation with test compound for 24 h. Slightly increased potency (up to 12-fold) was observed for (*R*)- and (*S*)-**11**, **47**, **52**, and tiotropium, illustrating the importance of incubation time when screening compounds that possess slow kinetics of binding. As expected, ipratropium potency under these conditions was unaffected due to its rapid binding kinetics. M_3 dissociation half-lives ($t_{1/2}$) determined under this revised incubation time (24 h) confirmed that all these agents (except ipratropium) exhibited very long residence time and potential for extended pharmacological effect.[2] The rapid dissociation half-life observed for ipratropium is in agreement with literature data.[26] The effect of these agents on airway smooth muscle was investigated in vitro using appropriate compound incubation times in isolated guinea pig tracheal (GPT) strips[27] and human bronchial rings. Potency within 10-fold of tiotropium was observed for (*R*)- and (*S*)-**11**, **47**, and **52** in GPT, along with very long-lasting DoA (T_{25} >16 h); remarkably, the time taken for the contractile response to recover by 25% following inhibition with compounds (*R*)- and (*S*)-**11**, **47**, and **52** was in excess of 16 h, indicating DoA that was at least tiotropium-like (T_{25} >12.9 h). Ipratropium was confirmed to be short-acting (T_{25} = 1.47 h). Human bronchus data indicated that **47** (pK_b = 9.6) was the most potent of these analogues and more importantly was also within 10-fold of tiotropium (pK_b = 10.2). This trend was also

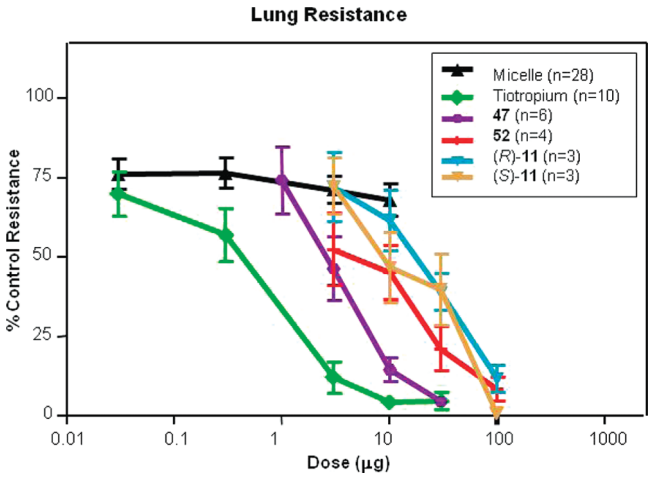

Figure 1. Lung resistance data in anaesthetized guinea pigs for (*R*)- and (*S*)-**11**, **47**, **52**, and tiotropium bromide, following cumulative intratracheal administration at hourly intervals, as solutions in micelle vehicle. ACh (iv) challenge was administered hourly (prior to the next escalating dose of compound) and the maximum increase in lung resistance recorded over a 5 min period. Data are expressed as a percentage of the pretreatment ACh (iv) control response (100%).

observed in vivo following lung resistance studies in anaesthetized guinea pigs (Figure 1 and Table 4). Overall, **47** was consistently the most attractive agent from these studies, possessing tiotropium-like DoA and potency within approximately 10-fold.

Compound **47** was subsequently profiled across human M_1-M_5 receptors to build a comprehensive picture of muscarinic pharmacology (Table 5). Binding affinity (K_i) determined with 24 h compound incubation demonstrated that **47** had balanced, potent activity across all M_1-M_5 receptors, similar to ipratropium and tiotropium. Dissociation half-life determined with 24 h compound incubation indicated that **47** possessed tiotropium-like kinetic selectivity for M_3 vs M_2 receptors.[2] This kinetic selectivity could be receptor rather than compound driven, as ipratropium has also been reported to show this kinetic behavior, albeit over a much shorter, less clinically relevant time frame.[26] Furthermore, with the exception of M_3 receptor dissociation half-life previously discussed, it appeared that **47** had a dissociation half-life shorter than that for tiotropium across M_1-M_5 receptors. Finally, the binding kinetics of **47** were investigated according the method of Motulsky and Mahan.[28] Interestingly, the off-rate (k_{off}) for **47** in this experiment was approximately 1 order of magnitude slower than that for tiotropium, confirming a very slow dissociation half-life ($t_{1/2}$ = 4998 min). The on-rate (k_{on}) for **47** was also slower than that for tiotropium and appeared consistent with previous in vitro observations. The resulting binding affinity for **47** (K_i = 0.0132 nM) was within 3-fold of that for tiotropium (K_i = 0.0057 nM), both of which were very potent in this assay and more potent than ipratropium, which was confirmed to have fast on-rate and off-rate.

With encouraging pharmacology in hand, we profiled **47** in a conscious dog model of bronchoconstriction to assess in vivo efficacy, DoA, and cardiovascular (CV) side effects (e.g., heart rate).[29] Dogs were treated with intratracheal (it.) solution administration of either M_3 antagonist or vehicle (micelle). Methacholine (MCh) challenge was administered it. to induce

Table 5. Pharmacological Effect of Compound 47 at Human Muscarinic M_1-M_5 Receptors in Vitro

	binding K_i[a] (nM)					dissociation $t_{1/2}$[b] (min)					M_3 binding kinetics[c]			
compd	M_1	M_2	M_3	M_4	M_5	M_1	M_2	M_3	M_4	M_5	K_i (nM)	k_{on} ($M^{-1}s^{-1}$)	k_{off} (s^{-1})	dissociation $t_{1/2}$ (min)
47	0.115	0.137	0.128	0.115	0.169	838	263	>1440	587	>1000	0.0132	1.05×10^7	1.39×10^{-4}	4998
	(n = 10)	(n = 6)	(n = 23)	(n = 2)	(n = 2)	(n = 7)	(n = 8)	(n = 8)	(n = 7)	(n = 8)	(n = 5)			
tiotropium	0.0130	0.0215	0.0098	0.0078	0.0266	>1430	>781	>1350	>1440	>1440	0.0057	2.12×10^8	1.22×10^{-3}	567.1
	(n = 57)	(n = 55)	(n = 340)	(n = 32)	(n = 29)	(n = 50)	(n = 45)	(n = 78)	(n ≥ 6)	(n = 60)	(n = 7)			
ipratropium	0.433	0.413	0.213	0.382	1.04	<15	<15	<15	<15	<39	0.157	1.00×10^9	1.60×10^{-1}	4.40
	(n = 62)	(n = 58)	(n = 348)	(n = 25)	(n = 25)	(n = 50)	(n = 44)	(n = 58)	(n = 47)	(n = 58)	(n = 7)			

[a] Binding affinity at human recombinant muscarinic M_1-M_5 receptors expressed in CHO cells following incubation with [^{3}H-NMS] and test compound for 24 h. [b] Test compound was incubated with CHO cells independently expressing the recombinant human M_1-M_5 receptors for 24 h at 100-fold the respective binding K_i, 90-fold dilution with buffer containing excess [^{3}H]-NMS followed. The dissociation half-life of the compound was measured by monitoring the association rate of [^{3}H]-NMS. [c] Binding affinity and kinetics determined by the method of Motulsky and Mahan.[28]

dx.doi.org/10.1021/jm200884j |*J. Med. Chem.* 2011, 54, 6888–6904

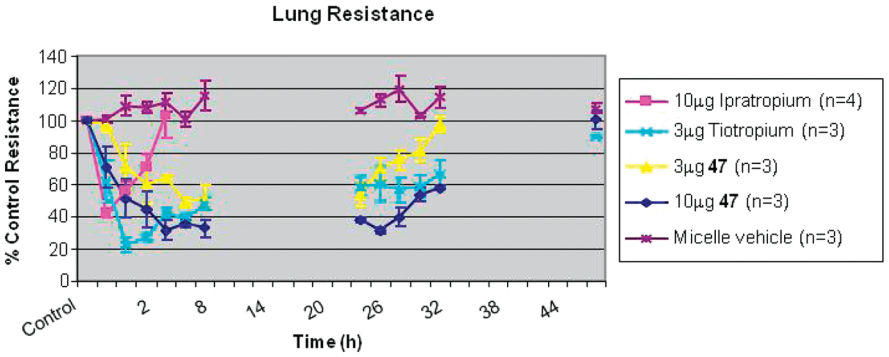

Figure 2. Lung resistance data in conscious dogs for **47**, ipratropium bromide, and tiotropium bromide, following intratracheal administration of a single dose, as a solution in micelle vehicle. MCh (it.) challenge was administered at 0.5 h, 1 h, and subsequently 2 h intervals, for up to 32 h, to measure the maximum increase in lung resistance, expressed as a percentage of the pretreatment MCh (it.) control response (100%).

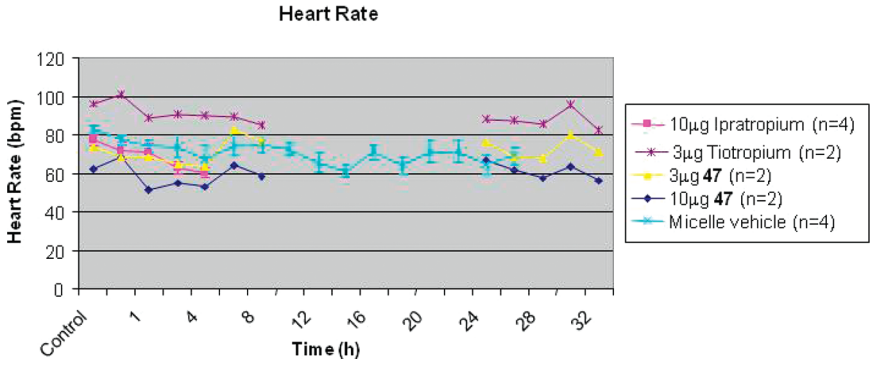

Figure 3. Heart rate data in conscious dogs for **47**, ipratropium bromide and tiotropium bromide following intratracheal administration of a single dose, as a solution in micelle vehicle. MCh (it.) challenge was administered at 0.5 h, 1 h and subsequently 2 h intervals, for up to 32 h, to measure CV parameters relative to the pretreatment MCh (it.) control response measured in that animal at the start of the study. Data are presented as heart rate, in beats-per-minute (bpm).

Table 6. In Vitro Permeability and in Vivo Pharmacokinetic Data for Compound 47

	in vitro permeability, MDCK-MDR1 P_{app} x 10^{-6} (cm/s)		rat in vivo PK, iv			
compd	A−B	B−A	V_d (L/kg)	Cl_T ((mL/min)/kg)	$t_{1/2}$ (h)	ppb (%)
47	7	64	8.4	134	0.9	93.5

an increase in lung resistance (R_L). R_L and CV parameters with antagonist treatment were compared to the control MCh response. In this model, **47** was found to be approximately 3-fold more potent (ID_{50} = 3.0 μg) than that for ipratropium (ID_{50} = 10.0 μg) but slightly less potent than that for tiotropium (ID_{50} < 3.0 μg) (Figure 2). At the ID_{50} dose (3.0 μg), **47** displayed long-lasting intrinsic DoA (>24 h) that was significantly superior to ipratropium (10.0 μg). Furthermore, a 3-fold higher dose of **47** (10 μg) afforded greater efficacy and DoA that was comparable to that for tiotropium (3.0 μg); both compounds were still efficacious 32 h postdose. Slower onset of action was observed for both doses of **47**, when compared to that for ipratropium and tiotropium. In vivo onset/DoA data for **47** appeared consistent with binding on-rate/off-rate kinetics observed in vitro (Table 5). Hemodynamic data from these studies confirmed that, relative to the control response measured in each animal at the start of the study, **47** (10 μg), ipratropium (10 μg), and tiotropium (3.0 μg) had no detectable CV effects up to 32 h postdose (Figure 3). These comparative data to clinical agents in a well validated in vivo model provided strong evidence that **47** would be able to deliver long-lasting (≥24 h) bronchodilation in humans from a projected once-daily inhaled dose of approximately 200 μg.

In vitro observations illustrated that **47** met our criteria of rapid CYP-mediated oxidative metabolism (Cl_{int} > 440 (μL/min)/mg) and phenolic glucuronidation (Cl_{int} > 221 (μL/min)/mg) (Table 2). Furthermore, in vitro permeability data in MDCK-MDR1 cells revealed that while **47** displayed high intrinsic permeability, it was also subject to very high transporter-mediated efflux (P_{app}(A−B) = 7 × 10^{-6} cm/s, P_{app}(B−A) = 64 × 10^{-6} cm/s), most likely as a substrate for P-glycoprotein (P-gp) (Table 6). Interestingly, the phenolic moiety appeared to be responsible for two of these observations: first, it introduced a site for extensive glucuronidation, and second, it induced significant P-gp efflux that was not observed for nonphenolic analogues (e.g., **25**; P_{app}(A−B) = 27 × 10^{-6} cm/s, P_{app}(B−A) = 28 × 10^{-6} cm/s). With desirable in vitro data predictive of low oral bioavailability (due to transporter limited absorption

dx.doi.org/10.1021/jm200884j |J. Med. Chem. 2011, 54, 6888–6904

Chart 3

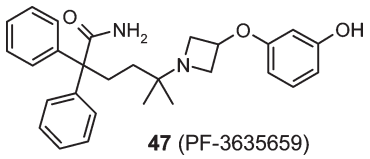

47 (PF-3635659)

through the gut lumen and high first pass metabolism), **47** was advanced to rat in vivo pharmacokinetic (PK) studies (Table 6).[30] Following iv administration, **47** exhibited rapid and extensive distribution (V_{dss} = 8.4 L/kg), very high unbound and total clearance (Cl_u = 2065 (mL/min)/kg, Cl_T = 134 (mL/min)/kg) that exceeded liver blood flow, and a short terminal half-life ($t_{1/2}$ = 0.9 h). Oral administration to rats resulted in no detectable systemic exposure, consistent with predictions from in vitro data.

The metabolites of **47** were found to be similar across a range of in vitro incubations in rat, dog, and human hepatocytes and liver microsomes. The major phase I metabolite from microsomal preparations was the azetidinol, resulting from O-dearylation. This metabolite was found to possess >10-fold weaker M_3 binding affinity (K_i = 1.64 nM) and much shorter M_3 dissociation half-life ($t_{1/2}$ = 69 min) than that for **47**, when assessed using these assays in their 24 h incubation format. In contrast, the major metabolite in hepatocytes was a phase II glucuronide, most likely the O-glucuronide from conjugation of the phenol group. Analysis of rat PK plasma samples showed that neither of these metabolites circulated in vivo to any meaningful extent. The primary enzyme-mediating phase I oxidative metabolism of **47** was found to be CYP3A4. Coincubation of human hepatocytes with the CYP3A4 inhibitor ketoconazole led to only a minor reduction (30%) in metabolism of **47**, again confirming extensive clearance of **47** by glucuronidation.

Overall, **47** exhibited an ideal pharmacokinetic profile for an inhaled agent by virtue of incomplete oral absorption (of the swallowed fraction) and high unbound clearance predicted in humans via oxidative metabolism and glucuronidation. Systemic exposure and associated adverse events in humans were therefore predicted to be minimal.[30] Furthermore, clinically relevant drug−drug interactions (DDI) were predicted to be minimal as a consequence of multiple routes of metabolism.

Subsequently, the hydrochloride salt form of **47** was isolated from ethanol and found to possess material properties that were consistent with our solid form requirements.[31] Analysis using well-known techniques such as PXRD, DSC, TGA, and DVS found **47** to be highly crystalline, anhydrous and nonhygroscopic (0.1% water uptake at 90% relative humidity) with high melting point (223 °C). The solid-state stability of **47** with lactose monohydrate (the most common carrier excipient used in commercial DPI) was demonstrated following storage of material blended at a 1:100 ratio for 28 days at 40 °C and 75% relative humidity. These material properties confirmed that **47** was compatible with inhaled administration from a DPI.

From a drug safety perspective, **47** demonstrated a safety margin in excess of 100-fold when evaluated for broader pharmacological activity against a wide ranging panel of in vitro assays representing receptors, enzymes, and ion channels. In vitro genetic toxicity testing and in vivo rat toleration studies were also completed without observing any meaningful adverse effects. Furthermore, **47** was inactive in a validated rabbit lung cough model following it. solution administration of doses up to 2000 μg.[32] These data provided preclinical confidence that **47** was unlikely to elicit cough in humans, thus addressing a key attrition risk for inhaled compound development and endorsing compound progression. Overall, **47** had a preclinical safety profile that suggested it should be well tolerated in humans at all clinically relevant inhaled doses.

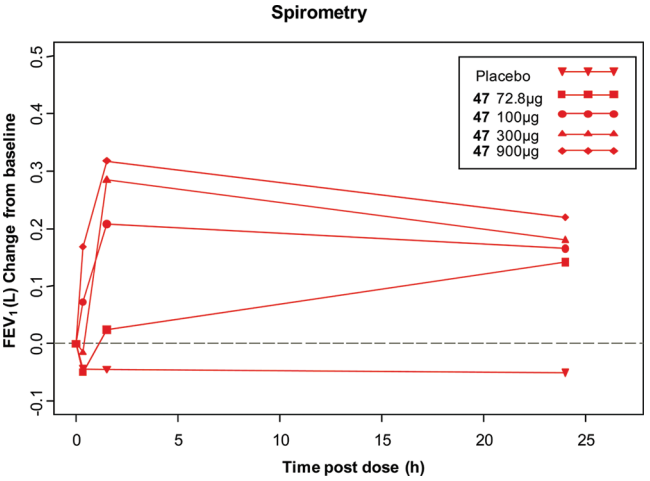

Figure 4. Phase I spirometry data in healthy human volunteers for **47**, following inhalation of dry-powder formulations. Data are expressed as the mean change in FEV_1 from baseline, by treatment.

CONCLUSION

In conclusion, we have described our "inhalation by design" strategy to deliver a novel muscarinic M_3 receptor antagonist (**47**) that has potential for once-daily inhaled administration in humans for the treatment of COPD. Geminal dimethyl functionality confers very long dissociative half-life (slow off-rate) from the M_3 receptor that mediates very long-lasting bronchodilation in vivo (≥24 h). Incorporation of the phenol moiety delivers extensive glucuronidation "by design" and negligible oral absorption, features that are complemented by rapid oxidative metabolism to provide **47** with an optimal preclinical PK profile for an inhaled agent. Material properties and projected once-daily inhaled dose size (~200 μg) are fully compatible with administration from a DPI delivery device. Furthermore, the preclinical safety profile of **47** suggests that it will be well tolerated in humans at all clinically relevant doses.

Successful delivery of this compelling profile ultimately identified **47** (PF-3635659) as a phase II clinical candidate (Chart 3). Spirometry data from healthy volunteers in phase I clinical studies illustrate that **47** provides efficacious 24 h bronchodilation (FEV_1 > 100 mL) from a single inhaled dose, thus confirming the suitability of **47** as a novel once-daily inhaled muscarinic M_3 receptor antagonist for the treatment of COPD (Figure 4). Human pharmacokinetic data from multidose phase I studies demonstrate very low levels of unbound systemic exposure at all doses (e.g., day 7, 200 μg dose, C_{maxu} = 0.008 nM), with no accumulation on repeat dosing, findings that are consistent with preclinical predictions. Safety (tachycardia) and toleration (dry mouth) data from multidose phase I studies indicate an adverse event profile that is at least noninferior to tiotropium bromide.

EXPERIMENTAL SECTION

Biology. In Vitro Potency at Recombinant Human M_3 Receptors Expressed in CHO Cells. M_3 potency was determined in CHO-K1 cells transfected with the NFAT-Betalactamase gene. The cells were resuspended at 2×10^5 cells/mL in growth medium, and 20 μL of this cell suspension was added to each well of a 384-well, black, clear-bottomed plate. The assay buffer used was PBS, supplemented with 0.05% Pluronic F-127 and 2.5% DMSO. Muscarinic M_3 receptor signaling was stimulated, in the presence and absence M_3 receptor antagonists, using 80 nM carbamyl choline incubated with the cells for 4 h at 37 °C/5% CO_2 and monitored at the end of the incubation period using a Tecan SpectraFluor+ plate reader (λ, excitation 405 nm, emission 450 and 503 nm). Inhibition curves were plotted and IC_{50} values generated using a four-parameter sigmoid fit and converted to K_i values using the Cheng−Prusoff correction and the K_D value for carbamyl choline in the assay.

In Vitro Binding Affinity at Recombinant Human M_1−M_5 Receptors Expressed in CHO Cells. Affinity and selectivity at human recombinant M_1−M_5 receptors, separately expressed in Chinese hamster ovary (CHO) cell membranes, were assessed using an *N*-methyl [^{3}H] scopolamine ([^{3}H]-NMS) filter binding assay similar to that previously described.[18] Briefly, CHO cell membranes were incubated in the presence or absence of test compounds and ^{3}H-NMS at room temperature for 2 or 24 h with shaking. The assay was terminated by rapidly filtering through GF/B Unifilter plates which were read on an NXT Topcount. Percent specific binding versus test compound concentration was plotted to determine an IC_{50} from a sigmoid curve using an in-house data analysis program. IC_{50} values were corrected to K_i values by applying the Cheng−Prussoff equation.

In Vitro Assessment of Dissociation Half-Life at Recombinant Human M_1−M_5 Receptors. Duration of action at M_1−M_5 receptors was assessed using a dilution−offset filter binding assay.[33] Briefly, the receptor was maximally occupied with the compound of interest, by incubating the membrane for 2 or 24 h with test compound at 100 × K_i. At various time points thereafter (between 15−1440 min) the mixture was diluted (90-fold), reducing the test compound concentration to 1 × K_i. This dilution was performed with assay buffer containing [^{3}H]-NMS, to give a final assay concentration of 12.5 × K_D. Therefore, the test compound was encouraged to dissociate from the receptor by both dilution and competition with [^{3}H]-NMS. Nonspecific binding was defined by 1 μM atropine, and total binding by equivalent DMSO (0.01%). Following 1440 min incubation, the assay was terminated by rapid filtration and the bound radioactivity quantified as described above. The association of [^{3}H]-NMS to the receptor was fitted to a generalized hyperbola, fixing the maximum to the maximum specific binding for the assay plate. The offset of the test compound was inferred from the association of [^{3}H]-NMS, expressed as the time taken to reach 50% of total [^{3}H]-NMS binding, for solvent-treated membranes. Offset values ($t_{1/2}$) were expressed as arithmetic means with 95% confidence intervals (CI). When the time to 50% recovery was estimated outside of the time points measured, results were quoted as >1440 or <15 min.

In Vitro Potency and Duration of Action in Guinea Pig Isolated Trachea. Tracheal strips (removed from male Dunkin−Hartley guinea pigs) were suspended in 5 mL of tissue baths under an initial tension of 1 g and bathed in warmed (37 °C), aerated (95% O_2/5% CO_2) Krebs solution containing 3 μM indomethacin and 10 μM guanethidine. At the end of the equilibration (1 h), tissues were electrically field stimulated (EFS) using the following parameters: 10 V, 10 Hz 0.1 ms pulse width with 10 s trains every 2 min. In each tissue a voltage response curve was constructed over the range 10−30 V (keeping all other stimulation parameters constant) to determine a just maximal stimulation. Using these stimulation parameters EFS responses were 100% nerve mediated and 100% cholinergic as confirmed by blockade by 1 μM tetrodotoxin or 1 μM atropine. Tissues were then repeatedly stimulated at 2 min intervals until the responses were reproducible.

(i) To assess potency (IC_{50}), the study compound was added to the tissue baths, with each tissue receiving a single concentration of compound and allowed to equilibrate for 8 h. At 8 h postaddition, the inhibition of the EFS response was recorded and IC_{50} curves were generated using a range of compound concentrations over tracheal strips from the same animal.

(i) To assess duration of action, the study compound was added for 2 h, the tissues were then rapidly washed, and the 1 mL/min perfusion with Krebs solution was re-established. Tissues were stimulated for a further 16 h, and recovery of the EFS response was recorded. At the end of the 16 h, 10 μM histamine was added to the baths to confirm tissue viability. The just maximal concentration (tested concentration giving a response >70% inhibition but less than 100%) of antagonist was identified from the IC_{50} curve, and the time to 25% recovery of the induced inhibition (T_{25}) was calculated in tissues receiving this concentration. Compounds are typically tested at n = 2−5 to estimate duration of action.

In Vivo Potency and Duration of Action in the Conscious Dog. Conscious male and female beagle dogs (10−15 kg) which had previously undergone a tracheostomy and esophagotomy were implanted with telemetry to continuously monitor arterial blood pressure (ABP), heart rate, myocardial contactility (change in left ventricular pressure (LVP) with time), and ECG. Flow was measured via a Fleisch tube and validyne attached to a trach tube placed in the tracheostomy. Pleural pressure was measured using a balloon catheter placed in the esophagotomy, linked to a pressure transducer. Total lung resistance and dynamic lung compliance (derived from flow and pulmonary pressure (PP)) were measured after each intratracheal methacholine (MCh) challenge. Following instrumentation and a 30 min stabilization period, nebulized MCh (1.0 mg/mL) was given to provide cardiovascular (CV) and respiratory parameters as a control response.

(i) For the dose−response study, doses of test compound or vehicle were given via intratracheal (it.) administration at cumulative 1 h intervals using a Penn-Century insufflator. Intratracheal MCh challenge was repeated 1 h posttest compound administration to compare airway resistance and CV parameters to the control MCh response.

(ii) For the duration of action studies, one dose of test compound or vehicle was administered intratracheally and MCh challenge (it.) repeated at 0.5 h, 1 h, and subsequently 2 h intervals for up to 32 h to compare airway resistance and CV parameters to the control MCh response.

Chemistry. Unless otherwise indicated, all reactions were carried out under a nitrogen atmosphere, using commercially available anhydrous solvents. Thin-layer chromatography was performed on glass-backed precoated Merck silica gel (60 F254) plates, and compounds were visualized using UV light, 5% aqueous potassium permanganate, or chloroplatinic acid/potassium iodide solution. Silica gel column chromatography was carried out using 40−63 μm silica gel (Merck silica gel 60). Ion exchange chromatography was performed using Isolute strong cation exchange resin (SCX-2) cartridges which had been prewashed with methanol. Proton NMR spectra were measured on a Varian Inova 400 or Varian Mercury 400 spectrometer in the solvents specified. In these NMR spectra, exchangeable protons that appeared distinct from solvent peaks are also reported. Low resolution mass spectra were recorded using the following system: PAL CAT sample injector; Agilent 1100 stack comprising of solvent degasser, pump and UV detector; Micromass ZQ 2000 MS detector with a scanning range of m/z 150−900. Test compound purity ≥95% was determined using combustion

analysis conducted by Exeter Analytical U.K. Ltd., Uxbridge, Middlesex, U.K. Tiotropium bromide was synthesized according to literature procedures.[34] Ipratropium bromide was purchased from Sigma.

5-Amino-5-methyl-2,2-diphenylhexanenitrile Hydrochloride Salt (37). A solution of diphenylacetonitrile (25.6 g, 132.3 mmol) in tetrahydrofuran (200 mL) was treated with potassium *tert*-butoxide (14.8 g, 132.3 mmol) and the resulting solution stirred for 10 min. A solution of *tert*-butyl 4,4-dimethyl-1,2,3-oxathiazinane-3-carboxylate 2,2-dioxide (**36**)[14] (35.1 g, 132.3 mmol) in tetrahydrofuran (300 mL) was then added over 15 min. The resulting solution was stirred for 4 h and then concentrated in vacuo. The residue was treated with 4 M hydrochloric acid in dioxane (165 mL, 661.5 mmol) and heated at 50 °C for 2 h. The solution was concentrated in vacuo to low volume, basified with saturated aqueous sodium carbonate solution, and extracted with dichloromethane (150 mL). The organic layer was dried (sodium sulfate) and concentrated in vacuo. The residue was treated with 4 M hydrochloric acid in dioxane (50 mL), concentrated in vacuo, and triturated with diethyl ether to give **37** as a solid, 36.2 g, 87% yield. ^{1}H NMR (400 MHz, CD_3OD) δ: 1.35 (s, 6H), 1.70−1.74 (m, 2H), 2.56−2.61 (m, 2H), 7.32−7.47 (m, 10H) ppm. LRMS: m/z 279 $[M + H]^+$.

5-(3-Hydroxyazetidin-1-yl)-5-methyl-2,2-diphenylhexanenitrile (38). A solution of amine hydrochloride salt **37** (22.1 g, 70.2 mmol) in dichloromethane (250 mL) was washed with saturated aqueous sodium carbonate solution (100 mL). The organic layer was dried (sodium sulfate) and concentrated in vacuo. The residue was dissolved in ethanol (250 mL) and treated with 2-chloromethyloxirane (7.8 g, 84.2 mmol), and the resulting solution was heated at 70 °C for 18 h. The mixture was cooled to room temperature and concentrated in vacuo. The residue was crystallized from toluene/pentane to give **38** as a solid, 18.1 g, 79% yield. ^{1}H NMR (400 MHz $CDCl_3$) δ: 0.92 (s, 6H), 1.31−1.36 (m, 2H), 2.42−2.46 (m, 2H), 2.88−2.97 (m, 2H), 3.29−3.37 (m, 2H), 4.31−4.38 (m, 1H), 7.27−7.43 (m, 10H) ppm. LRMS: m/z 335 $[M + H]^+$.

Methanesulfonic Acid 1-(4-Cyano-1,1-dimethyl-4,4-diphenylbutyl)azetidin-3-yl Ester (39). A solution of hydroxyazetidine **38** (15.0 g, 44.9 mmol) in pyridine (150 mL) at −15 °C was treated dropwise with methanesulfonyl chloride (10.4 mL, 134.6 mmol) over 15 min. The resulting solution was stirred at 0−5 °C for 3 h. The mixture was quenched with saturated aqueous sodium hydrogen carbonate solution (150 mL) and extracted with ethyl acetate (2 × 150 mL). The combined organic layers were dried (sodium sulfate) and concentrated in vacuo. The residue was redissolved in toluene (100 mL) and the solvent removed in vacuo to give **39** as a gum, 18.6 g, 100% yield. ^{1}H NMR (400 MHz, $CDCl_3$) δ: 0.92 (s, 6H), 1.29−1.33 (m, 2H), 2.41−2.45 (m, 2H), 2.98 (s, 3H), 3.21−3.24 (m, 2H), 3.37−3.41 (m, 2H), 4.96−5.01 (m, 1H), 7.26−7.40 (m, 10H) ppm. LRMS: m/z 413 $[M + H]^+$.

5-[3-(3-Methoxyphenoxy)azetidin-1-yl]-5-methyl-2,2-diphenylhexanenitrile (40). A solution of mesylate **39** (12.3 g, 29.8 mmol) in acetonitrile (150 mL) was treated with 3-methoxyphenol (3.9 mL, 35.8 mmol) and potassium carbonate (10.3 g, 74.5 mmol). The resulting mixture was stirred at 80 °C for 3.5 h. The mixture was cooled to room temperature and concentrated in vacuo, and the residue was partitioned between ethyl acetate (250 mL) and saturated aqueous sodium hydrogen carbonate solution (150 mL). The aqueous layer was separated and extracted with ethyl acetate (2 × 200 mL). The combined organic layers were washed with brine (300 mL), dried (sodium sulfate), and concentrated in vacuo to give **40** as a brown oil, 16.2 g, 69% yield. ^{1}H NMR (400 MHz, $CDCl_3$) δ: 0.95 (s, 6H), 1.31−1.44 (m, 2H), 2.41−2.56 (m, 2H), 3.07−3.24 (m, 2H), 3.42−3.54 (m, 2H), 3.77 (s, 3H), 4.63−4.74 (m, 1H), 6.28−6.38 (m, 2H), 6.48−6.55 (m, 1H), 7.26−7.49 (m, 11H) ppm. LRMS: m/z 441 $[M + H]^+$.

5-[3-(3-Hydroxyphenoxy)azetidin-1-yl]-5-methyl-2,2-diphenylhexanamide (47, PF-3635659). A solution of nitrile **40** (13.4 g, 30.4 mmol) in 3-methylpentan-3-ol (150 mL) was treated with potassium hydroxide (34.1 g, 608 mmol), and the resulting solution was stirred at 120 °C for 18 h. The mixture was cooled to room temperature and concentrated in vacuo, and the residue was partitioned between ethyl acetate (200 mL) and water (200 mL). The organic layer was separated, washed with water (200 mL), dried (sodium sulfate), and concentrated in vacuo. The residue was purified by column chromatography on silica gel, eluting with ethyl acetate/methanol/0.88 specific gravity ammonia (90:10:1, by volume) to give 5-[3-(3-methoxyphenoxy)-azetidin-1-yl]-5-methyl-2,2-diphenylhexanamide as a white foam, 10.7 g, 77% yield. ^{1}H NMR (400 MHz, $CDCl_3$) δ: 0.92 (s, 6H), 1.12−1.23 (m, 2H), 2.40−2.50 (m, 2H), 3.10−3.25 (m, 2H), 3.44−3.58 (m, 2H), 3.78 (s, 3H), 4.62−4.72 (m, 1H), 6.30−6.38 (m, 2H), 6.47−6.54 (m, 1H), 7.10−7.18 (m, 1H), 7.22−7.45 (m, 10H) ppm. LRMS: m/z 459 $[M + H]^+$.

A solution of 5-[3-(3-methoxyphenoxy)azetidin-1-yl]-5-methyl-2,2-diphenylhexanamide (9.0 g, 19.6 mmol) in dichloromethane (1.25 L) at 0 °C was treated dropwise with 1 M boron tribromide in dichloromethane (58.9 mL, 58.9 mmol). The resulting mixture was warmed to room temperature with stirring over 2 h. The mixture was recooled to 0 °C, quenched with addition of 1 M aqueous sodium hydroxide solution (200 mL), and allowed to warm to room temperature over 1 h. The aqueous layer was separated and extracted with ethyl acetate (2 × 200 mL). The combined organic layers were dried (sodium sulfate) and concentrated in vacuo. The residue was purified by column chromatography on silica gel, eluting with (dichloromethane/methanol/0.88 specific gravity ammonia (90:10:1, by volume))/pentane (50:50, by volume) to give **47** as a white foam, 3.40 g, 39% yield. ^{1}H NMR (400 MHz, $CDCl_3$) δ: 1.10 (s, 6H), 1.22−1.34 (m, 2H), 2.42−2.55 (m, 2H), 3.28−3.40 (m, 2H), 3.65−3.88 (m, 2H), 4.70−4.80 (m, 1H), 5.55−5.70 (bs, 2H), 6.23−6.36 (m, 2H), 6.45−6.53 (m, 1H), 7.03−7.12 (m, 1H), 7.19−7.39 (m, 10H) ppm. LRMS: m/z 443 $[M - H]^-$, 445 $[M + H]^+$. Anal. ($C_{28}H_{32}N_2O_3 \cdot 1.0H_2O$) C, H, N. HPLC analysis: ≥98.5% purity.

■ ASSOCIATED CONTENT

Supporting Information. Biology experimental section for the in vitro human bronchus assay, in vivo anaesthetized guinea pig model, and in vivo rabbit lung Aδ-fiber cough model; chemistry experimental details and analytical data for intermediates **1**−**3**, (*R*)- and (*S*)-**5**, (*S*)-**6**, (*R*)- and (*S*)-**7**, (*S*)-**8**, (*R*)- and (*S*)-**10**, (*R*)- and (*S*)-**12**−**14**, (*S*)-**17**, (*R*)-**18**, **23**, **24**, **28**−**31**, **33**, **34**, **41**−**46**, **54**, **56**−**63**, and test compounds **4**, (*R*)- and (*S*)-**9**, (*R*)- and (*S*)-**11**, (*S*)-**15**, (*S*)-**16**, (*S*)-**19**, (*R*)-**20**, **25**, **26**, **32**, **35**, **48**−**53**, **55**, **64**. This material is available free of charge via the Internet at http://pubs.acs.org.

■ AUTHOR INFORMATION

Corresponding Author

*(P.G.) Phone: +441304812980; e-mail: paglossop@gmail.com. (C.W.) Phone: +441223847005; e-mail: christine.watson100@gmail.com.

Present Addresses

[#]Pfizer Global Research and Development, Eastern Point Rd., Groton, CT 06340.

[¥]Pfizer, 2002 Executive Suite, 200 Cambridge Park Dr., Cambridge, MA 02140.

[Δ]Peakdale Chemistry Services, Ramsgate Rd, Sandwich, Kent CT13 9NJ, U.K.

[‖]MedImmune, Milstein Building, Granta Park, Cambridge, CB21 6GH, U.K.

■ ACKNOWLEDGMENT

We thank Michele Coghlan, Stuart Marshall, Sheena Patel, Jo Ann Rhodes, and Jessica Watson for their contributions to in vitro biology studies, and John Adcock, Tim Davies, James Philip, Louise Sladen, and Karen Wright for in vivo biology studies. We also thank Katie Bainbridge, Trish Costello, David Cox, Steve Denton, David Fengas, Ben Greener, Tim Hobson, Simon Mantell, Louise Marples, and Keith Reeves for assistance with the chemistry program. Dzelal Serdarevic is also thanked for the provision of clinical data.

■ ABBREVIATIONS USED

ACh, acetyl choline; CCh, carbamyl choline; CHO, Chinese hamster ovary; COPD, chronic obstructive pulmonary disease; CYP, cytochrome P450; DDI, drug−drug interaction; DoA, duration of action; DPI, dry powder inhaler; DSC, differential scanning calorimetry; DVS, dynamic vapor sorption; EFS, electrical field stimulation; FEV_1, forced expiratory volume in 1 s; GPT, guinea pig trachea; IT, intratracheal; LAAC, long-acting anticholinergic; LAMA, long-acting muscarinic antagonist; MCh, methacholine; NADPH, reduced form of nicotinamide adenine dinucleotide phosphate; NMS, *N*-methylscopolamine; PXRD, powder X-ray diffraction; R_L, lung resistance; TGA, thermogravimetric analysis; TI, therapeutic index; UDPGA, uridine-5′-diphosphoglucuronic acid; UGT, uridine-5′-diphosphoglucuronosyl transferase

■ REFERENCES

(1) Rabe, K. F.; Hurd, S.; Anzueto, A.; Barnes, P. J.; Buist, S. A.; Calverley, P.; Fukuchi, Y.; Jenkins, C.; Rodriguez-Roisin, R.; van Weel, C.; Zielinski, J. Global Strategy for the Diagnosis, Management, and Prevention of Chronic Obstructive Pulmonary Disease: GOLD Executive Summary. *Am. J. Respir. Crit. Care Med.* **2007**, *176*, 532–555.

(2) Hansel, T. T.; Barnes, P. J. Tiotropium bromide: A novel once-daily anticholinergic bronchodilator for the treatment of COPD. *Drugs Today* **2002**, *38*, 585–600.

(3) Gross, N. J.; Skorodin, M. S. Role of the Parasympathetic System in Airway Obstruction Due to Emphysema. *N. Eng. J. Med.* **1984**, *311*, 421–425.

(4) Coulson, F. R.; Fryer, A. D. Muscarinic acetylcholine receptors and airway diseases. *Pharmacol. Ther.* **2003**, *98*, 59–69.

(5) Joos, G. F. Potential for long-acting muscarinic antagonists in chronic obstructive pulmonary disease. *Expert. Opin. Investig. Drugs* **2010**, *19*, 257–264.

(6) Lainé, D. I. Long-acting muscarinic antagonists for the treatment of chronic obstructive pulmonary disease. *Expert Rev. Clin. Pharmacol.* **2010**, *3*, 43–53.

(7) Cazzola, M.; Matera, M. G. Emerging inhaled bronchodilators: an update. *Eur. Respir. J.* **2009**, *34*, 757–769.

(8) Villetti, G.; Pastore, F.; Bergamaschi, M.; Bassani, F.; Bolzoni, P. T.; Battipaglia, L.; Amari, G.; Rizzi, A.; Delcanale, M.; Volta, R.; Cenacchi, V.; Cacciani, F.; Zaniboni, M.; Berti, F.; Rossoni, G.; Harrison, S.; Petrillo, P.; Santoro, E.; Scudellaro, R.; Mannini, F.; Geppetti, P. A.; Razzetti, R.; Patacchini, R.; Civelli, M. Bronchodilator Activity of (3*R*)-3-[[[(3-Fluorophenyl)[(3,4,5-trifluorophenyl)methyl]amino]carbonyl]-oxy]-1-[2-oxo-2-(2-thienyl)ethyl]-1-azoniabicyclo[2.2.2]octane Bromide (CHF5407), a Potent, Long-Acting, and Selective Muscarinic M_3 Receptor Antagonist. *J. Pharmacol. Exp. Ther.* **2010**, *335*, 622–635.

(9) (a) Wan, Z.; Laine, D. I.; Yan, H.; Zhu, C.; Widdowson, K. L.; Buckley, P. T.; Burman, M.; Foley, J. J.; Sarau, H. M.; Schmidt, D. B.; Webb, E. F.; Belmonte, K. E.; Palovich, M. Discovery of (3-*endo*)-3-(2-cyano-2,2-diphenylethyl)-8,8-dimethyl-8-azoniabicyclo[3.2.1]octane bromide as an efficacious inhaled muscarinic acetylcholine receptor antagonist for the treatment of COPD. *Bioorg. Med. Chem. Lett.* **2009**, *19*, 4560–4562. (b) Lainé, D. I.; Wan, Z.; Yan, H.; Zhu, C.; Xie, H.; Fu, W.; Busch-Petersen, J.; Neipp, C.; Davis, R.; Widdowson, K. L.; Blaney, F. E.; Foley, J.; Bacon, A. M.; Webb, E. F.; Luttmann, M. A.; Burman, M.; Sarau, H. M.; Salmon, M.; Palovich, M. R.; Belmonte, K. Design, Synthesis, and Structure−Activity Relationship of Tropane Muscarinic Acetylcholine Receptor Antagonists. *J. Med. Chem.* **2009**, *52*, 5241–5252.

(10) Prat, M.; Fernández, D.; Buil, M. A.; Crepso, M. I.; Casals, G.; Ferrer, M.; Tort, L.; Castro, J.; Monleón, J. M.; Gavaldà, A.; Miralpeix, M.; Ramos, I.; Doménech, T.; Vilella, D.; Antón, F.; Huerta, J. M.; Espinosa, S.; López, M.; Sentellas, S.; González, M.; Albertí, J.; Segarra, V.; Cárdenas, A.; Beleta, J.; Ryder, H. Discovery of Novel Quaternary Ammonium Derivatives of (3*R*)-Quinuclidinol Esters as Potent and Long-Acting Muscarinic Antagonists with Potential for Minimal Systemic Exposure after Inhaled Administration: Identification of (3*R*)-3-{[Hydroxy(di-2-thienyl)acetyl]oxy}-1-(3-phenoxypropyl)-1-azoniabicyclo[2.2.2]octane Bromide (Aclidinium Bromide). *J. Med. Chem.* **2009**, *52*, 5076–5092.

(11) Cazzola, M. Aclidinium bromide, a novel long-acting muscarinic M3 antagonist for the treatment of COPD. *Curr. Opin. Invest. Drugs* **2009**, *10*, 482–490.

(12) Haeberlin, B.; Stowasser, F.; Wirth, W.; Baumberger, A.; Abel, S.; Kaerger, S.; Kieckbusch, T. Compositions of glycopyrronium salt for inhalation. PCT Int. Appl. Publ. WO 2008000482, 2008.

(13) Denton, S. M.; Wood, A. A Modified Bouveault Reaction for the Preparation of α,α-Dimethylamines from Amides. *Synlett* **1999**, *1*, 55–56.

(14) Boehringer, M.; Hunziker, D.; Kuehne, H.; Loeffler, B. M.; Sarabu, R.; Wessel, H. P. *N*-substituted Pyrrolidine Derivatives as Dipeptidyl Peptidase IV Inhibitors. PCT Int. Appl. Publ. WO 2003037327, 2003.

(15) Espino, C. G.; Wehn, P. M.; Chow, J.; Du Bois, J. Synthesis of 1,3-Difunctionalized Amine Derivatives through Selective C−H Bond Oxidation. *J. Am. Chem. Soc.* **2001**, *123*, 6935–6936.

(16) Bower, J. F.; Švenda, J.; Williams, A. J.; Charmant, J. P. H.; Lawrence, R. M.; Szeto, P.; Gallagher, T. Cyclic Sulfamidates as Vehicles for the Synthesis of Substituted Lactams. *Org. Lett.* **2004**, *6*, 4727–4730.

(17) Glossop, P. A.; Mantell, S. J.; Strang, R. S.; Watson, C. A. L.; Wood, A. Carboxamide derivatives as muscarinic receptor antagonists. PCT Int. Appl. Publ. WO 2007034325, 2007.

(18) (a) Casarosa, P.; Bouyssou, T.; Germeyer, S.; Schnapp, A.; Gantner, F.; Pieper, M. Preclinical Evaluation of Long-Acting Muscarinic Antagonists: Comparison of Tiotropium and Investigational Drugs. *J. Pharmacol. Exp. Ther.* **2009**, *330*, 660–668. (b) Gavaldà, A.; Miralpeix, M.; Ramos, I.; Otal, R.; Carreño, C.; Viñals, M.; Doménech, T.; Carcasona, C.; Reyes, B.; Vilella, D.; Gras, J.; Cortijo, J.; Morcillo, E.; Llenas, J.; Ryder, H.; Beleta, J. Characterization of Aclidinium Bromide, a Novel Inhaled Muscarinic Antagonist, with Long Duration of Action and a Favorable Pharmacological Profile. *J. Pharmacol. Exp. Ther.* **2009**, *331*, 740–751.

(19) (a) Cross, P. E.; Mackenzie, A. R. Preparation of pyrrolidine derivatives as muscarinic receptor antagonists. Eur. Pat. Appl. Publ. EP388054, 1990. (b) Alabaster, V. A. Discovery and development of selective M_3 antagonists for clinical use. *Life Sci.* **1997**, *60*, 1053–1060.

(20) Lee, J. T.; Kroemer, H. K.; Silberstein, D. J.; Funck-Brentano, C.; Lineberry, M. D.; Wood, A. J.; Roden, D. M.; Woosley, R. L. The Role of Genetically Determined Polymorphic Drug Metabolism in the Beta-Blockade Produced by Propafenone. *New Engl. J. Med.* **1990**, *322*, 1764–1768.

(21) Williams, J. A.; Hyland, R.; Jones, B. C.; Smith, D. A.; Hurst, S.; Goosen, T. C.; Peterkin, V.; Koup, J. R.; Ball, S. E. Drug-Drug Interactions for UDP-Glucuronosyltransferase Substrates: A Pharmacokinetic Explanation for Typically Observed Low Exposure (AUC_I/AUC) Ratios. *Drug Metab. Dispos.* **2004**, *32*, 1201–1208.

(22) Glossop, P. A.; Lane, C. A. L.; Price, D. A.; Bunnage, M. E.; Lewthwaite, R. A.; James, K.; Brown, A. D.; Yeadon, M.; Perros-Huguet, C.; Trevethick, M. A.; Clarke, N. P.; Webster, R.; Jones, R. M.; Burrows, J. L.; Feeder, N.; Taylor, S. C. J.; Spence, F. J. Inhalation by Design:

Novel Ultra-Long-Acting β_2-Adrenoreceptor Agonists for Inhaled Once-Daily Treatment of Asthma and Chronic Obstructive Pulmonary Disease That Utilize a Sulfonamide Agonist Headgroup. *J. Med. Chem.* **2010**, *53*, 6640–6652.

(23) Boase, S.; Miners, J. O. In vitro-in vivo correlations for drugs eliminated by glucuronidation: Investigations with the model substrate zidovudine. *Br. J. Clin. Pharmacol.* **2002**, *54*, 493–503.

(24) Magdalou, J.; Fournel-Gigleux, S.; Ouzzine, M. Insights on membrane topology and structure/function of UDP-glucuronosyltransferases. *Drug Metab. Rev.* **2010**, *42*, 159–166.

(25) Copeland, R. A.; Pompliano, D. L.; Meek, T. D. Drug-target residence time and its implications for lead optimization. *Nature Rev. Drug Discov.* **2006**, *5*, 730–739.

(26) Disse, B.; Reichl, R.; Speck, G.; Traunecker, W.; Rominger, K. L.; Hammer, R. Ba 679 BR, A novel long-acting anticholinergic bronchodilator. *Life Sci.* **1993**, *52*, 537–544.

(27) Nials, A. T.; Sumner, M. J.; Johnson, M.; Coleman, R. A. Investigations into factors determining the duration of action of the beta 2-adrenoceptor agonist, salmeterol. *Br. J. Pharmacol.* **1993**, *108*, 507–515.

(28) Motulsky, H. J.; Mahan, L. C. The Kinetics of Competitive Radioligand Binding Predicted by the Law of Mass Action. *Mol. Pharmacol.* **1984**, *25*, 1–9.

(29) Wright, K.; Davies, T.; Clarke, N.; Yeadon, M.; Perros-Huguet, C. PF-00610355 – an inhaled β_2-adrenoceptor agonist with superior potency and duration of action (DoA) to salmeterol in the conscious dog model of bronchoconstriction. *Eur. Respir. J.* **2009**, *34* (S53), Abstract P2060.

(30) Taburet, A. M.; Schmit, B. Pharmacokinetic Optimization of Asthma Treatment. *Clin. Pharmacokinet.* **1994**, *26*, 396–418.

(31) Glossop, P. A.; James, K. The hydrochloride salt of 5-(3-(3-hydroxyphenoxy)azetidin-1-yl)-5-methyl-2,2-diphenylhexanamide and its use as a medicament. PCT Int. Appl. Publ. WO 2008135819, 2008.

(32) Sladen, L.; Wright, K.; Adcock, J.; Chaffe, P.; Clarke, N.; Yeadon, M.; Perros-Huguet, C. Effects of intra tracheal PF-00610355, an inhaled β_2-adrenoceptor agonist, in anaesthetised animals. *Eur. Respir. J.* **2009**, *34* (S53), Abstract P2020.

(33) Watson, J.; Strawbridge, M.; Brown, R.; Campany, K.; Coghlan, M.; Trevethick, M. Offset rates of tiotropium and ipratropium at human recombinant muscarinic M_1-M_5 receptors using a dilution-offset methodology. *Fundam. Clin. Pharmacol.* **2008**, *22* (S2), 78, Abstract P102.

(34) Banholzer, R.; Bauer, R.; Reichl, R. Preparation of anticholinergic scopine, (nor)tropine, and granatoline esters of thienylcarboxylic acids and their quaternary salts. Eur. Pat. Appl. Publ. EP 418716, 1991.